CrispEdit: Low-Curvature Projections for Scalable Non-Destructive LLM Editing

Zarif Ikram, **Arad Firouzkouhi**, **Stephen Tu**, **Mahdi Soltanolkotabi**, **Paria Rashidinejad**
{zikram,firouzko,stephen.tu,soltanol,paria.rashidinejad}@usc.edu

University of Southern California

A central challenge in large language model (LLM) editing is capability preservation: methods that successfully change targeted behavior can quietly game the editing proxy and corrupt general capabilities, producing degenerate behaviors reminiscent of proxy/reward hacking. We present CrispEdit, a scalable and principled second-order editing algorithm that treats capability preservation as an explicit constraint, unifying and generalizing several existing editing approaches. CrispEdit formulates editing as constrained optimization and enforces the constraint by projecting edit updates onto the low-curvature subspace of the capability-loss landscape. At the crux of CrispEdit is expressing capability constraint via *Bregman divergence*, whose quadratic form yields the Gauss–Newton Hessian exactly and even when the base model is not trained to convergence. We make this second-order procedure efficient at the LLM scale using Kronecker-factored approximate curvature (K-FAC) and a novel *matrix-free projector* that exploits Kronecker structure to avoid constructing massive projection matrices. Across standard model-editing benchmarks, CrispEdit achieves high edit success while **keeping capability degradation below 1%** on average across datasets, significantly improving over prior editors.

Date: February 17, 2026
Website: https://crispedit.github.io
Code: https://github.com/zarifikram/CrispEdit

USC

1 Introduction

Large language models (LLMs) are rapidly becoming a shared backbone for knowledge work, spanning search and question answering (Gao et al., 2023b; Lewis et al., 2020), science (Jumper et al., 2021), software development (Chen, 2021), decision support (Lopez-Lira and Tang, 2023), and education (Kasneci et al., 2023). Yet every day, facts shift, new discoveries land, products ship, hallucinations or unsafe behaviors are uncovered, quickly making the models stale. Retraining from scratch is the cleanest way to absorb this drift, but it is also the most expensive and slowest. Model editing (Sinitsin et al., 2020; De Cao et al., 2021; Mitchell et al., 2022b; Wang et al., 2024c) offers a practical alternative: apply targeted updates to correct a fact, insert new knowledge, remove unsafe behavior, personalize the style *while leaving everything else intact*.

In many cases, edits may appear to succeed while quietly degrading broader capabilities reminiscent of reward/proxy hacking (Gao et al., 2023a). This degradation can manifest as brittle reasoning, weaker instruction-following, or even broken fluency. In response, prior work

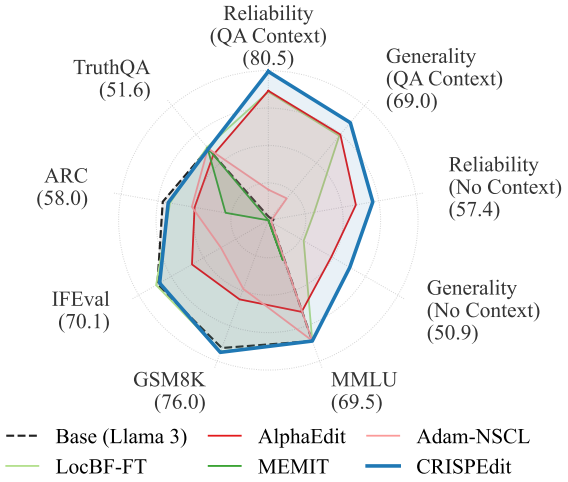

Figure 1 Comparison overview of CrispEdit. CrispEdit achieves strong edit reliability and generality, with and without QA context, while preserving broad base capabilities (MMLU, GSM8K, IFEval, ARC-C, TruthfulQA) on LLaMA-3-8B-Instruct.

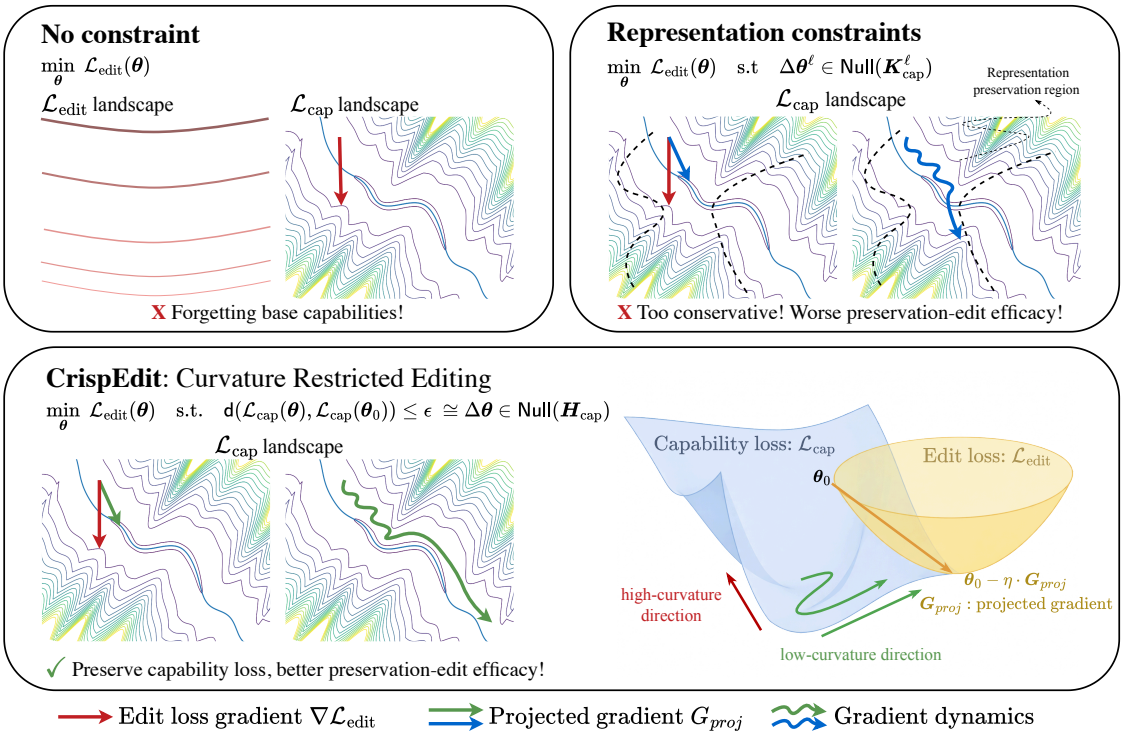

Figure 2 Geometric interpretation of CrispEdit compared to baseline editing strategies. *Top left:* Standard gradient descent effectively minimizes edit loss but moves perpendicular to the capability contours, resulting in high capability loss (degradation). *Top right:* Projecting onto the nullspace of activation covariance is overly conservative; it preserves representations but restricts the update too heavily to successfully optimize the edit loss. *Bottom:* CrispEdit projects the update onto the low-curvature subspace of the capability loss. This allows changes in representations to satisfy the edit while moving along the "valley" of the landscape to maintain general model capabilities.

has introduced heuristic guardrails: restrict updates to a small set of parameters (Hu et al., 2022; Yu et al., 2024), localize "where the knowledge lives," (Meng et al., 2022; Yang et al., 2025b; Gu et al., 2025) or constrain representation changes (e.g., via subject-centric "knowledge vectors") (Meng et al., 2023; Fang et al., 2025). Despite improvements, these methods tend to bake in strong assumptions about edit structure (e.g., explicit subjects/entities) and impose constraints in parameter or representation space that are only indirectly tied to capability preservation, resulting in a poor edit–preservation trade-off. Indeed, editors built on such constraints still perform poorly when tested *in the wild* under natural autoregressive generation, despite looking strong under unrealistic teacher-forced evaluation that scaffolds the ground-truth prefix and target length (Yang et al., 2025a).

In this paper, we adopt a first-principles formulation of model editing: an edit should reduce an edit loss while leaving broader capabilities effectively unchanged. Accordingly, we pose editing as a constrained optimization problem that seeks to minimize the edit loss subject to negligible changes in capability loss, measured on a designated capability set via a distance metric (Section 2). Standard approaches that replace the constraint with a soft penalty typically require nontrivial tuning and can be prohibitively expensive when the capability set is far larger than the edit set. This motivates us to ask: *How to enforce capability preservation directly, without turning editing into full retraining?*

To address this, we introduce CrispEdit (Curvature-Restricted In-Situ Parameter Editing), a scalable non-destructive editor, built around the following core ideas.

1. Preserving capabilities with low-curvature projections. A core idea behind CrispEdit is that not all parameter directions are equally important for preserving a model's capabilities. Recent work shows that the curvature of the pretrained loss landscape can be characterized by the Hessian, which is observed to be highly anisotropic: sharp in a small number of directions and flat in others (Sagun et al., 2017; Oymak et al.,

2019; Ghorbani et al., 2019; Kalra et al., 2026). CrispEdit exploits this structure by projecting updates into low-curvature subspaces of Hessian, effectively "hiding" parameter movement where capabilities are minimally affected (see Figure 2 and Section 3.1).

2. Avoiding base model convergence requirement with Bregman constraint. A quadratic approximation based on the standard Hessian—which instantiates our formulation with a Euclidean distance—requires assuming that the base model is trained to (near)-convergence, which is rarely satisfied in practice for modern large networks. We resolve this by measuring capability preservation using *Bregman divergence*. This choice yields a quadratic form expressed exactly in terms of the *Gauss-Newton Hessian* (GNH), even when the base model is not trained to convergence, avoiding stationarity assumptions.

3. Representation constraints as a restrictive special case. Our Bregman-GNH formulation also sheds light on several successful prior heuristics. We prove (see Proposition 1) popular editors such as AlphaEdit (Fang et al., 2025) and Adam-NSCL (Wang et al., 2021) solve an approximate special case of our framework, but do so within *far more restrictive* and lower-dimensional subspaces, leading to a worse capability preservation-edit tradeoff (Figure 1).

4. Scalable matrix-free low-curvature projectors. The remaining challenge is scale: how can we efficiently compute and store curvature information for billion-parameter transformers? CrispEdit addresses this with two key ideas:

(a) The resulting GNH is amenable to accurate approximations via Kronecker-factored approximate curvature (Martens and Grosse, 2015, K-FAC), which we leverage to enable efficient computation of the low-curvature projection matrix.

(b) Instead of explicitly constructing a low-curvature projection matrix, we introduce (Section 3.3) a matrix-free projector that exploits the Kronecker eigen-structure: rotate gradients into a factored eigenbasis, mask high-curvature components, and rotate back. This makes constraint-aware second-order editing feasible and enables precomputing capability curvature statistics once and reusing them across many future edits, amortizing cost and enabling batch and sequential editing.

Experimental results. We evaluate CrispEdit in both small- and large-scale regimes. In controlled small-scale experiments on image classification (MNIST $\mapsto$ FashionMNIST), where calculating exact curvature is feasible, we show that Hessian low-curvature projections yield the strongest capability preservation, and that K-FAC closely tracks this behavior cheaply. We then scale CrispEdit to edit LLMs (e.g., LLaMA-3-8B-Instruct and Qwen-2.5-1.5B-Instruct) and evaluate them as used in practice: edits should be *reliable* in standalone autoregressive generations, *generalize* across semantically equivalent in-scope queries, and remain *local*, preserving out-of-scope knowledge and broad skills such as reasoning, instruction-following, and truthfulness. We further test our method in both *batch* editing, where many edits are applied at once, and *sequential* editing, where batches of edits are applied to the model sequentially. Across settings, CrispEdit consistently improves the edit–capability trade-off, achieving strong edit success while substantially reducing capability degradation, with modest compute and storage requirements.[1]

2 The Model editing problem

Let $f_{\boldsymbol{\theta}} : \mathcal{X} \mapsto \mathcal{Y}$ denote a model with parameters $\boldsymbol{\theta} \in \Theta \subseteq \mathbb{R}^p$, mapping inputs $x \in \mathcal{X}$ to outputs $y \in \mathcal{Y}$. Model editing seeks to update a pretrained (base) model $f_{\boldsymbol{\theta}_0}$ with initial parameters $\boldsymbol{\theta}_0$, using a provided edit target pair $(x, y) \in \mathcal{X} \times \mathcal{Y}$, while preserving the existing capabilities of the base model. We formalize this as follows.

Let $\mathcal{D}_{\text{cap}} = \{(x_i, y_i)\}_{i=1}^n$ be a reference dataset that serves as a proxy for capabilities we wish to preserve, an exemplar of the domains on which the model should continue to perform well. We formulate capability preservation through the empirical loss

$$\mathcal{L}_{\text{cap}}(\boldsymbol{\theta}; \mathcal{D}_{\text{cap}}) := \frac{1}{n} \sum_{i=1}^{n} \ell(f_{\boldsymbol{\theta}}(x_i), y_i),$$

[1] Using cached curvature, 3000 edits with our method takes six minutes on an NVIDIA A40 GPU.

where $\ell(\hat{y}, y)$ is a task-appropriate loss (e.g., cross entropy). Preserving capabilities then means keeping $\mathcal{L}(\boldsymbol{\theta}; \mathcal{D}_{\text{cap}})$ close to its pre-edit value, i.e., $\mathcal{L}(\boldsymbol{\theta}; \mathcal{D}_{\text{cap}}) \approx \mathcal{L}(\boldsymbol{\theta}_0; \mathcal{D}_{\text{cap}})$. Let $\mathcal{D}_{\text{edit}} = \{(x_i, y_i)\}_{i=1}^{T}$ be the edit dataset containing the desired edit pairs. We write $\mathcal{L}_{\text{edit}}(\boldsymbol{\theta}; \mathcal{D}_{\text{edit}})$ to denote an edit loss, such as the negative log-likelihood of edit outputs. Using the language of constrained optimization, a natural optimization problem that expresses our desire to minimize edit loss subject to preserving capabilities is the following:[2]

$$\min_{\boldsymbol{\theta} \in \Theta} \ \mathcal{L}_{\text{edit}}(\boldsymbol{\theta}) \quad \text{s.t.} \quad \mathsf{d}\left(\mathcal{L}_{\text{cap}}(\boldsymbol{\theta}), \mathcal{L}_{\text{cap}}(\boldsymbol{\theta}_0)\right) \leq \varepsilon, \tag{1}$$

where $\mathsf{d}(\cdot, \cdot)$ is a measure of distance, such as the difference between the two loss values or the Bregman divergence, and ε is a small tolerance value. The above formulation is general, unifying and extending many existing model editing frameworks as we discuss in Section 5.

While Problem (1) rigorously expresses our desired intent for model editing, actually solving (1), especially at LLM scale, is challenging due to the hard constraint. We note that we focus on the constrained formulation above in lieu of the standard Lagrangian relaxation to (1), namely $\min_{\boldsymbol{\theta} \in \Theta} \ \mathcal{L}_{\text{edit}}(\boldsymbol{\theta}) + \lambda \mathsf{d}\left(\mathcal{L}_{\text{cap}}(\boldsymbol{\theta}), \mathcal{L}_{\text{cap}}(\boldsymbol{\theta}_0)\right)$. This is due to the fact that in typical operating regimes n (the number of reference pairs) far exceeds T (the number of edits), and the computational overhead of gradient-based optimization on the unconstrained problem can be non-trivial. We avoid this complexity by considering an alternative approach to approximating (1) based on low-curvature projections.

3 CrispEdit: Curvature-Restricted In-Situ Parameter Editing

We now present CrispEdit for solving Problem (1). The key idea is to edit only along directions that are locally "safe" for maintaining capabilities as informed by the constraint. We start in Section 3.1 with a simple instantiation of CrispEdit under the standard capability loss difference and derive a principled curvature-restricted model-editing algorithm. Then, in Section 3.2, we leverage *Bregman divergences* to derive a practical editing approach that scales to billion-parameter LLMs.

For what follows, we assume that both the maps $\hat{y} \mapsto \ell(\hat{y}, y)$ and $\boldsymbol{\theta} \mapsto f_{\boldsymbol{\theta}}(x)$ are twice continuously differentiable over their respective domains. This immediately holds for architectures with smooth activation functions such as GeLU/SwiGLU. Furthermore, this assumption can readily be relaxed to functions that are twice differentiable except on a measure zero set, such as architectures with ReLU activations; for simplicity of exposition, we omit these details.

3.1 Preserving capabilities with low-curvature updates

We first consider the distance measure to be the standard distance $\mathsf{d}(a, b) = |a - b|$. Furthermore, in this section, we assume that the base parameters $\boldsymbol{\theta}_0$ are a local minima of the capabilities loss $\mathcal{L}_{\text{cap}}(\boldsymbol{\theta})$; we remove this assumption in Section 3.2 by using a different distance measure. Applying a second-order Taylor expansion to the constraint in (1) yields $\mathcal{L}_{\text{cap}}(\boldsymbol{\theta}) - \mathcal{L}_{\text{cap}}(\boldsymbol{\theta}_0) \approx \frac{1}{2}(\boldsymbol{\theta} - \boldsymbol{\theta}_0)^\top \boldsymbol{H}_{\text{cap}}(\boldsymbol{\theta} - \boldsymbol{\theta}_0)$, where $\boldsymbol{H}_{\text{cap}} \coloneqq \nabla^2_\theta \mathcal{L}_{\text{cap}}(\boldsymbol{\theta}_0)$ is the Hessian of the capability loss function evaluated at $\boldsymbol{\theta}_0$, and the first term in Taylor expansion is zero because $\nabla_\theta \mathcal{L}_{\text{cap}}(\boldsymbol{\theta}_0) = 0$. Under this setting, (1) can be approximated by optimizing the following quadratically constrained optimization problem:

$$\min_{\boldsymbol{\theta} \in \Theta} \ \mathcal{L}_{\text{edit}}(\boldsymbol{\theta}) \quad \text{s.t.} \quad (\boldsymbol{\theta} - \boldsymbol{\theta}_0)^\top \boldsymbol{H}_{\text{cap}}(\boldsymbol{\theta} - \boldsymbol{\theta}_0) \leq \varepsilon. \tag{2}$$

In the deep learning literature, it is well-understood that in typical overparameterized settings, the Hessian $\boldsymbol{H}_{\text{cap}}$ at the end of training is usually low-rank (Sagun et al., 2017; Oymak et al., 2019; Ghorbani et al., 2019). Thus, the ellipsoidal constraint in (2) offers many parameter directions around $\boldsymbol{\theta}_0$ of *low-curvature*, where the capability loss $\mathcal{L}_{\text{cap}}$ remains (approximately) invariant. These low-curvature directions enable the optimization (2) to decrease the edit loss $\mathcal{L}_{\text{edit}}$, while limiting loss of capabilities. Furthermore, compared to the Lagrange relaxation objective, the quadratic constraint offers several key advantages:

(a) *Strict control of capability loss:* The ellipsoidal constraint can be enforced via projected gradient or trust-region methods, enabling strict control of tolerated capability degradation; we discuss this shortly.

[2] We will drop the dependency of the capabilities and edit losses on datasets $\mathcal{D}_{\text{edit}}$ and $\mathcal{D}_{\text{cap}}$ when it is clear from the context.

(b) *Scalability to billion-parameter models:* The second-order relaxation of the constraint forms the foundation for efficiently scaling our approach to billion-parameter LLMs leveraging Bregman divergences (cf. Section 3.2).
(c) *Pre-computation:* The curvature model $\boldsymbol{H}_{\text{cap}}$ can be precomputed once and reused across many subsequent edits, amortizing cost and enabling sequential and online interventions (cf. Section 3.4).

Projected low-curvature gradient descent. We can enforce the constraint in (2) by ensuring that the weight changes $\Delta\boldsymbol{\theta} = \boldsymbol{\theta} - \boldsymbol{\theta}_0$ are in the (approximate) null-space of the Hessian $\boldsymbol{H}_{\text{cap}}$, i.e., $\boldsymbol{H}_{\text{cap}}\Delta\boldsymbol{\theta} \approx 0$ which is equivalent to $\Delta\boldsymbol{\theta} \in \mathsf{Null}(\boldsymbol{H}_{\text{cap}})$. A sufficient condition to enforce the constraint during gradient descent is projecting the gradients to the approximate null-space of $\boldsymbol{H}_{\text{cap}}$ at every gradient step.

Let $\boldsymbol{H}_{\text{cap}} = \boldsymbol{U}\boldsymbol{\Sigma}\boldsymbol{U}^\top$ be the eigen-decomposition of $\boldsymbol{H}_{\text{cap}}$, where $\boldsymbol{\Sigma} = \mathsf{diag}(\sigma_1, \ldots, \sigma_p)$ and $\sigma_1 \geq \ldots \geq \sigma_p \geq 0$ (recall that $\boldsymbol{\theta}_0$ is locally optimal). We construct a low-curvature projector by discarding the top eigenspace. Concretely, given an energy threshold $\gamma \in (0, 1)$, let $k := \min\{r \in [p] \mid \sum_{i=1}^{r} \sigma_i / \sum_{i=1}^{p} \sigma_i \geq \gamma\}$ denote the minimum index capturing γ-fraction of the eigenspectrum. Then, the orthogonal projection to the *remaining* directions $\boldsymbol{U}_{>k} := [u_{k+1} \mid \ldots \mid u_p]$ can be computed as:

$$\boldsymbol{g}_t^{\text{proj}} = \boldsymbol{P}_\gamma \nabla_{\boldsymbol{\theta}} \mathcal{L}_{\text{edit}}(\boldsymbol{\theta}_t), \quad \text{where} \quad \boldsymbol{P}_\gamma := \boldsymbol{U}_{>k}\boldsymbol{U}_{>k}^\top. \tag{3}$$

Intuitively, the projection in (3) removes the components of the edit gradient that point in the directions where capability loss is sensitive. We will refer to the subspace spanned by $\boldsymbol{U}_{>k}$ as the γ-approximate nullspace.

3.2 Gauss-Newton constraint via Bregman divergence

In Section 3.1 and deriving (2), we assumed that $\nabla_{\boldsymbol{\theta}} \mathcal{L}_{\text{cap}}(\boldsymbol{\theta}_0) = 0$. However, in training neural networks, especially LLMs, one typically does not train the network to convergence, to avoid overfitting. Moreover, the capability loss can only be viewed as a mere *proxy* to the pretraining loss. To avoid relying on the linear term vanishing, we instantiate CrispEdit using a *Bregman divergence* that is always first-order flat at $\boldsymbol{\theta}_0$.

Definition 1 (**Bregman divergence**). *For a pair (x, y) and loss $\ell(\cdot, \cdot)$, define the Bregman divergence:*

$$\mathsf{d}_{\ell,y}^{Breg}(f_{\boldsymbol{\theta}}(x), f_{\boldsymbol{\theta}_0}(x)) := \ \ell(f_{\boldsymbol{\theta}}(x), y) - \ell(f_{\boldsymbol{\theta}_0}(x), y) - \langle \nabla \ell(f_{\boldsymbol{\theta}_0}(x), y),\ f_{\boldsymbol{\theta}}(x) - f_{\boldsymbol{\theta}_0}(x) \rangle\,.$$

With this definition, we now consider a distance defined as $\mathsf{d}(\mathcal{L}_{\text{cap}}(\boldsymbol{\theta}), \mathcal{L}_{\text{cap}}(\boldsymbol{\theta}_0)) := \frac{1}{n}\sum_{i=1}^{n} \mathsf{d}_{\ell,y_i}^{\text{Breg}}(f_{\boldsymbol{\theta}}(x_i), f_{\boldsymbol{\theta}_0}(x_i))$. A key property of Bregman divergence is that in the second-order Taylor approximation, the gradient is zero for any fixed $\boldsymbol{\theta}$, resulting in the following (cf. Appendix B):

$$\mathsf{d}_{\ell}^{\text{Breg}}(\mathcal{L}_{\text{cap}}(\boldsymbol{\theta}), \mathcal{L}_{\text{cap}}(\boldsymbol{\theta}_0)) \approx \frac{1}{2}(\boldsymbol{\theta} - \boldsymbol{\theta}_0)^\top \boldsymbol{G}_{\text{cap}}(\boldsymbol{\theta} - \boldsymbol{\theta}_0),$$

where $\boldsymbol{G}_{\text{cap}}$ is the Gauss-Newton Hessian (GNH, also referred to as the Generalized Gauss-Newton), defined as $\boldsymbol{G}_{\text{cap}} := \mathbb{E}_{\mathcal{D}_{\text{cap}}}\left[\boldsymbol{J}^\top \boldsymbol{H}_{\hat{y}} \boldsymbol{J}\right]$. Here, $\boldsymbol{J} = \nabla_{\boldsymbol{\theta}} f_{\boldsymbol{\theta}}(x)$ is the network's parameter-output Jacobian, and $\boldsymbol{H}_{\hat{y}} = \nabla_{\hat{y}}^2 \ell$ is the Hessian of the loss with respect to the network's outputs, with the expectation taken empirically over the dataset $\mathcal{D}_{\text{cap}}$. Importantly, $\boldsymbol{G}_{\text{cap}}$ is well-behaved for overparameterized and partially trained networks, and lends itself to reliable and scalable approximations which we explore below.

Connections to existing model editing methods. It turns out many existing heuristic model editing methods can be viewed as solving the problem (2) via conservative approximations of the quadratic constraint, and with more restrictive assumptions. For example, the popular AlphaEdit technique (Fang et al., 2025) (and related methods like Adam-NSCL (Wang et al., 2021)) can be viewed as solving the following approximate optimization problem:

$$\min_{\boldsymbol{\theta}}\ \mathcal{L}_{\text{edit}}(\boldsymbol{\theta}) \quad \text{s.t.} \quad \boldsymbol{\theta} - \boldsymbol{\theta}_0 \in \mathsf{Null}(\boldsymbol{K}_{\text{cap}}). \tag{4}$$

Here, matrix $\boldsymbol{K}_{\text{cap}}$ is constructed from the so-called *knowledge vectors* for *a particular* MLP layer, used for preserving capabilities in certain domains of interest. We show that AlphaEdit solves a special, more restrictive problem compared to our approach; the proof can be found in Appendix C.

Proposition 1 (**AlphaEdit is more conservative**). *Fix an MLP layer l and consider updating only the weights of layer l. Let $\boldsymbol{K}_{cap}^{l} \coloneqq \boldsymbol{I} \otimes [\boldsymbol{a}_{l-1}^{1}, \ldots, \boldsymbol{a}_{l-1}^{n}]$ be the layer-input activations on the capability dataset, and $\boldsymbol{G}_{cap}^{l}$ be the GNH. Then,* $\mathsf{Null}(\boldsymbol{K}_{cap}^{l}) \subseteq \mathsf{Null}(\boldsymbol{G}_{cap}^{l})$.

Unlike AlphaEdit's representation-level restriction via $\boldsymbol{K}_{\text{cap}}$, our method preserves capabilities through loss curvatures via $\boldsymbol{G}_{\text{cap}}$. Furthermore, our approach can update multiple layers simultaneously, whereas AlphaEdit edits one layer at a time; consequently, a direct comparison requires matching the edited parameter subset. Proposition 1 shows that even if we artificially restrict our method to a single layer l, the feasible update subspace defined by the corresponding layerwise GNH is a *superset* of AlphaEdit's layerwise subspace. We emphasize that this constraint of the form can be significantly more restrictive than our approach. In particular, $\mathsf{Null}(\boldsymbol{K}_{\text{cap}})$ can be a subspace of *much smaller dimension* than the nullspace of the GNH. Furthermore, in contrast to the knowledge matrix, in practice, the GNH is known to be flat in many directions, e.g., due to network overparameterization (Sagun et al., 2017; Oymak et al., 2019). Therefore, the constraint in AlphaEdit can be significantly more restrictive, leading to a worse tradeoff between preserving prior capabilities and applying the new edits, as evidenced by our comparative analysis in Section 4.2.

Result: Representational constraint is a restrictive special case of our formulation

We prove that heuristic methods like AlphaEdit enforce updates within the nullspace of layer inputs ($\boldsymbol{K}_{\text{cap}}$), which is a strict subset of the nullspace of the loss curvature ($\boldsymbol{G}_{\text{cap}}$) utilized by our method. Consequently, AlphaEdit solves a significantly more constrained optimization problem, limiting its accessible parameter space and resulting in a worse tradeoff between editing efficacy and capability preservation.

3.3 K-FAC for scalable, matrix-free projections

The remaining obstacle is scale: $\boldsymbol{G}_{\text{cap}}$ is expensive to compute and represent as a matrix. To address this, we approximate $\boldsymbol{G}_{\text{cap}}$ with Kronecker-Factored Approximate Curvature (K-FAC)[3] (Martens and Grosse, 2015; George et al., 2018). At a high level, K-FAC approximates $\boldsymbol{G}_{\text{cap}}$ as a block-diagonal matrix, i.e., $\boldsymbol{G}_{\text{cap}} \approx \text{blkdiag}(\boldsymbol{G}_{\text{cap}}^{1}, \ldots, \boldsymbol{G}_{\text{cap}}^{L})$ for a network with L layers. To describe each block-diagonal approximation, suppose that layer l of an MLP computes its outputs as follows: $\boldsymbol{s}_l = \boldsymbol{W}_l \boldsymbol{a}_{l-1}$ and $\boldsymbol{a}_l = \phi_l(\boldsymbol{s}_l)$, where $\boldsymbol{a}_{l-1} \in \mathbb{R}^{d_{\text{in}}}$ are input activations, $\boldsymbol{W}_l \in \mathbb{R}^{d_{\text{out}} \times d_{\text{in}}}$ are layer weights (including any bias terms), and $\boldsymbol{s}_l \in \mathbb{R}^{d_{\text{out}}}$ are layer pre-activations. Let $\boldsymbol{g}_l = \nabla_{\boldsymbol{s}_l} \log p(\hat{y} \mid x)$ denote the pseudo-gradients of preactivations. Then, the K-FAC approximation of GNH for layer l is given by:

$$\boldsymbol{G}_{\text{cap}}^{l} \approx \mathbb{E}\left[\boldsymbol{a}_{l-1}\boldsymbol{a}_{l-1}^{\top}\right] \otimes \mathbb{E}\left[\boldsymbol{g}_l \boldsymbol{g}_l^{\top}\right] \coloneqq \boldsymbol{A}_{l-1} \otimes \boldsymbol{S}_l. \tag{5}$$

Here, $\boldsymbol{A}_{l-1}$ and $\boldsymbol{S}_l$ are uncentered covariance matrices of the activations and preactivation pseudo-gradients, respectively, with the expectation taken with respect to the capabilities dataset $\mathcal{D}_{\text{cap}}$. This reduces the per-layer storage requirements from $O(d_{\text{in}}^2 d_{\text{out}}^2)$ to $O(d_{\text{in}}^2 + d_{\text{out}}^2)$ memory.

Matrix-free projections without forming $\boldsymbol{P}_{\gamma}^{(l)}$. Even with K-FAC approximations in place, explicitly materializing a projector matrix $\boldsymbol{P}_{\gamma}^{(l)}$ for the γ-approximate nullspace of $\boldsymbol{G}_{\text{cap}}^{(l)}$ is memory-prohibitive. Thus, we now describe an efficient method to project onto the γ-approximate nullspace that does not require explicitly forming $\boldsymbol{P}_{\gamma}^{(l)}$. The key idea behind our approach is the fact that the eigenvalues/eigenvectors of a Kronecker product $\boldsymbol{M} \otimes \boldsymbol{N}$ are simply the product of the eigenvalues/eigenvectors of $\boldsymbol{M}$ and $\boldsymbol{N}$. Specifically, let $\boldsymbol{A}_{l-1} = \boldsymbol{U}_{\text{in}} \boldsymbol{\Lambda}_{\text{in}} \boldsymbol{U}_{\text{in}}^{\top}$ and $\boldsymbol{S}_{l-1} = \boldsymbol{U}_{\text{out}} \boldsymbol{\Lambda}_{\text{out}} \boldsymbol{U}_{\text{out}}^{\top}$ denote the respective eigendecompositions of $\boldsymbol{A}_{l-1}$ and $\boldsymbol{S}_{l-1}$. We show in Appendix D, for a weight-gradient $\boldsymbol{Q}_l = \nabla_{\boldsymbol{W}_l} L_{\text{edit}}(\boldsymbol{\theta})$, the projected gradient $\boldsymbol{Q}_l^{\text{proj}} = \text{mat}(\boldsymbol{P}_{\gamma}^{(l)} \text{vec}(\boldsymbol{Q}_l))$ can be written as:

$$\boldsymbol{Q}_l^{\text{proj}} \;=\; \boldsymbol{U}_{\text{out}} \Big((\boldsymbol{U}_{\text{out}}^{\top} \boldsymbol{Q}_l \boldsymbol{U}_{\text{in}}) \odot \boldsymbol{M} \Big) \boldsymbol{U}_{\text{in}}^{\top}, \tag{6}$$

where $\odot$ denotes the Hadamard (entry-wise) matrix product and $\boldsymbol{M}_{ij} = \mathbf{1}\left[\lambda_i^{\text{out}} \lambda_j^{\text{in}} \leq \lambda_{\gamma}\right]$ is a binary mask that selects low-curvature components of the Kronecker matrix; λ_{γ} denotes the largest eigenvalue associated

[3]While K-FAC approximates the Fisher information matrix, for many models, such as the transformers with softmax output and cross-entropy loss, it is equivalent to the GNH (Martens, 2020).

Algorithm 1 CRISPEDIT

Require: $\boldsymbol{\theta}_0$, $\mathcal{D}_{\text{cap}}$, $\mathcal{D}_{\text{edit}}$, number of epochs E.
Ensure: Edited model parameters $\boldsymbol{\theta}$.

```
Compute K-FAC factors (A_{l-1}, S_l) for all finetuned layers l on L(θ; D_cap); cache U_out^(l), U_in^(l), and projection mask M^(l) for each layer (computed via SVD).
Initialize parameters θ ← θ_0.
for e = 1 to E do
    for each minibatch B ⊂ D_edit do
        Compute gradient Q_l for each fine-tuned layer l.
        Project gradient to Q_l^proj (cf. Equation (6))
        Update parameters θ using Q_l^proj.
    end for
end for
```

with the γ-approximate nullspace of $\boldsymbol{P}_\gamma^\ell$. Using this formula, one never needs to form the $d_{\text{in}}d_{\text{out}} \times d_{\text{in}}d_{\text{out}}$ projector, further reducing the storage requirement from $O(d_{\text{in}}^2 d_{\text{out}}^2)$ to $O(d_{\text{in}}^2 + d_{\text{out}}^2 + d_{\text{in}}d_{\text{out}})$. With this projection in hand, we are ready to define CRISPEDIT, presented in Algorithm 1.

Result: K-FAC enables scalable matrix-free curvature projection.

Directly storing the GNH or its projector is memory-prohibitive. We overcome this by approximating the GNH with K-FAC and deriving a *matrix-free* projection update. By exploiting the Kronecker structure, we project gradients using only the eigendecompositions of the smaller factor matrices $\boldsymbol{A}$ and $\boldsymbol{S}$, avoiding the materialization of the full high-dimensional projector. This reduces memory complexity from $O(d_{\text{in}}^2 d_{\text{out}}^2)$ to $O(d_{\text{in}}^2 + d_{\text{out}}^2)$, enabling CRISPEDIT to scale efficiently.

3.4 Sequential editing via online projection updates

Up to this point, we have described CRISPEDIT in a *batch editing setting*, where we assume all the edits $\mathcal{D}_{\text{edit}}$ are gathered at once, and the base model is updated to incorporate all the edits. A complementary setting is one of *sequential editing*, where edits (single instances or batches) arrive over time and the model is updated from $f_{\boldsymbol{\theta}_0}$ to $f_{\boldsymbol{\theta}_1}, \ldots, f_{\boldsymbol{\theta}_K}$ in K successive rounds. Here, at every round k, the goal is to preserve both the base capabilities and the earlier edits in rounds 1 to $k-1$ applied to the model. This setting is closely connected to continual (or lifelong) learning (De Lange et al., 2021; Shi et al., 2025) and inherits its core failure mode catastrophic forgetting. Batch editing can be viewed as "breadth-first", integrating many edits at once, whereas sequential editing is "depth-first", repeatedly revising the model as the new edit data arrive (Yang et al., 2025b).

Concretely, consider a sequence of edit data that arrives over time in chunks: $\mathcal{D}_{\text{edit}}^{(1)}, \ldots, \mathcal{D}_{\text{edit}}^{(K)}$. A naïve algorithm at every round k sets $\mathcal{D}_{\text{edit}} = \cup_{i=1}^{k} \mathcal{D}_{\text{edit}}^{(i)}$, and approximately solves problem (1) using Algorithm 1.

Algorithm 2 CRISPEDIT-SEQ

Require: $\boldsymbol{\theta}_0$, $\mathcal{D}_{\text{cap}}$, edits $\mathcal{D}_{\text{edit}}^{(1)}, \ldots, \mathcal{D}_{\text{edit}}^{(K)}$.
Ensure: Edited models $\boldsymbol{\theta}_1, \ldots, \boldsymbol{\theta}_K$ (updated sequentially).

```
Compute K-FAC factors {A^(l-1), S^(l)} on L(θ; D_cap).
Initialize {A_acc^(l-1), S_acc^(l)} ← {A_cap^(l-1), S_cap^(l)}.
for k = 1 to K do
    Solve (1) for θ_k with edit loss L(θ; D_edit^(k)), using layer-wise γ-approximate nullspace projections induced by {A_acc^(l-1), S_acc^(l)} (cf. Algorithm 1).
    Compute K-FAC factors {A_edit,k^(l-1), S_edit,k^(l)} for D_edit^(k).
    Aggregate K-FAC factors {A_acc^(l-1), S_acc^(l)} with {A_edit,k^(l-1), S_edit,k^(l)} via streaming averages.
end for
```

However, this naïve approach must keep all edits around, which can be infeasible and/or impractical for large K or privacy-sensitive settings (Yao et al., 2023). To address these issues, we develop an algorithm (Algorithm 2) which sequentially maintains the requisite statistics to implement γ-approximate nullspace projection. The key idea behind Algorithm 2 is that the $\boldsymbol{A}_{l-1}$ and $\boldsymbol{S}_l$ factors from K-FAC (cf. (5)) are memory-efficient sufficient statistics to summarize the approximate nullspace of the capability loss and the previous edit losses. By updating these statistics online after each round k, we can simultaneously minimize $\mathcal{L}(\boldsymbol{\theta}; \mathcal{D}_{\text{edit}}^{(k)})$ while treating both capabilities and the existing edit losses as hard constraints.

4 Experiments

4.1 Comparison of various second-order constraints

To understand the effect of various second-order constraints on capability preservation in model editing, we consider a simple setting where calculating the Hessian of the model is tractable. Since this is prohibitive for large LLMs, we use LeNet-5 (LeCun et al., 2002) as a representative model. We pre-train the model to 99% test accuracy on the MNIST dataset (LeCun, 1998) and fine-tune it on the Fashion-MNIST dataset (Xiao et al., 2017). In this setting, we treat the MNIST loss as the capabilities objective, and the Fashion-MNIST loss as the edit objective.

For the fine-tuning phase, we first compute the γ-approximate nullspace projector of the Hessian of the pre-train loss, applying projected gradient descent (PGD) to fine-tune a one hidden-layer MLP, as described in Section 3.1. To address the inaccuracy of the projector caused by parameter drift, we recalculate the γ-approximate nullspace projector every time parameter changes more than 25%. To understand the trade-off curve between pre-train and fine-tune test accuracy, we sweep over a range of energy threshold $\gamma = 1 - 10^{-k}$ with $k \in [\frac{1}{10}, 7]$. We then compare this algorithm against running PGD onto four alternative approximate nullspaces: (a) activation covariance (cf. Adam-NSCL (Wang et al., 2021)), (b) Gauss-Newton Hessian, (c) K-FAC (Martens and Grosse, 2015), and (d) eigenvalue-corrected K-FAC (EK-FAC) (George et al., 2018).

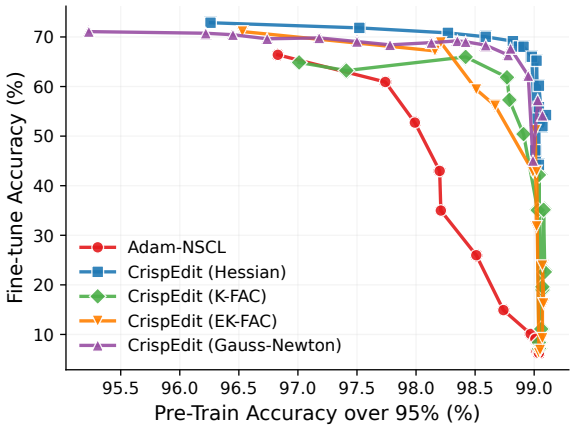

Figure 3 Tradeoff between pre-training accuracy (capability preservation) and post-training performance (edit efficacy) for different nullspace projection methods. We fine-tune a LeNet-5 model pre-trained on MNIST on Fashion-MNIST in the γ-approximate nullspace of the embeddings (Adam-NSCL) Hessian along with Hessian approximations Gauss-Newton Hessian, K-FAC, and EK-FAC (CrispEdit), over a range of energy thresholds γ.

Our results, which illustrate the trade-off between pre-train and fine-tune performance for both the Hessian-based algorithm and the four alternatives (a)-(d), are shown in Figure 3. We highlight three findings: (i) Projecting gradient updates onto the γ-approximate nullspace of the Hessian provides an effective strategy for improving fine-tune accuracy on Fashion-MNIST while maintaining base MNIST performance. (ii) The GNH approach yields a trade-off curve that is quite competitive with the Hessian approach, illustrating the efficacy of the Bregman constraint. This, however, is not the case with the activation covariance used by Adam-NSCL. (iii) Both K-FAC and EK-FAC approximate the performance of the GNH approach reasonably well. The last point (iii) is promising, as it suggests that using K-FAC when we are unable to compute the full Hessian (e.g., LLMs) is a viable approach as we demonstrate next.

4.2 Large-scale LLM evaluations

We now study scaling CrispEdit to billion-parameter LLMs, predominately focusing on LLaMA-3-8B-Instruct. We investigate the following: (i) How well can we edit the model? (ii) Do the edits generalize for different

Table 1 Comparison of CrispEdit with existing methods on editing LLaMA-3-8B-Instruct. *Rel* and *Gen* denote reliability and generalization. We edit 3,000 samples from three datasets, evaluate edits with WILD, and measure base capability on five benchmarks. Values that are best or within 5% of best are in bold.

Data	Method	Edited Capabilities				Base Capabilities					Time
		QA Context		No Context							
		Rel	Gen	Rel	Gen	MMLU	IFEval	TruthfulQA	ARC-C	GSM8K	
ZsRE	LLaMA-3-8B-Instruct	2.1	1.7	2.9	2.1	69.5	69.3	50.7	58.0	73.5	
	MEMIT	0.1	0.0	0.1	0.1	22.9	0.0	51.3	23.5	0.0	9h 27m
	AlphaEdit	70.1	60.6	48.1	39.4	52.7	47.7	46.3	40.5	45.5	7h 19m
	Adam-NSCL	16.6	15.5	1.9	2.0	**69.2**	29.6	50.8	42.0	39.5	29m 19s
	LocBF-FT	69.5	59.7	25.2	22.1	**69.5**	**70.1**	51.6	**54.0**	**75.5**	22m 15s
	UltraEdit	20.0	16.3	22.7	17.4	**69.3**	**72.5**	51.8	**54.5**	**73.0**	3m 23s
	MEND	0.0	0.0	0.0	0.0	22.9	18.2	0.0	26.0	0.0	58m 20s
	FT	46.8	43.1	9.9	8.3	**69.3**	45.0	48.7	43.0	50.0	4m 32s
	FT Sequential	3.6	3.5	0.9	1.2	**68.8**	19.4	52.8	40.5	6.5	9m 17s
	LoRA	9.1	7.4	18.7	7.2	**67.8**	**70.8**	52.0	**56.0**	71.0	47m 24s
	LoRA Sequential	4.4	4.0	1.3	0.9	**67.3**	64.6	**56.0**	47.0	67.0	3h 12m
	CrispEdit	**80.5**	**69.0**	57.4	50.9	**69.5**	67.9	50.5	**55.0**	**76.0**	4m 6s
	CrispEdit-Seq	71.1	62.9	**72.8**	**60.6**	**67.8**	**70.2**	**53.6**	52.0	**74.0**	43m 36s
CounterFact	LLaMA-3-8B-Instruct	1.2	1.0	0.3	0.6	69.5	69.3	50.7	58.0	73.5	
	MEMIT	0.0	0.0	0.0	0.0	24.6	18.6	49.6	21.0	0.0	7h 30m
	AlphaEdit	74.9	**57.0**	**50.5**	**44.1**	47.4	32.9	41.5	40.5	37.5	5h 56m
	Adam-NSCL	19.1	8.5	1.7	1.8	**68.6**	22.8	**57.1**	39.5	16.5	24m 9s
	LocBF-FT	61.1	41.6	10.9	13.3	**69.4**	65.0	51.3	**52.5**	**74.0**	14m 40s
	UltraEdit	18.1	12.4	10.2	9.3	**69.2**	**68.6**	49.2	**52.0**	**74.0**	3m 9s
	MEND	0.0	0.0	0.0	0.0	22.9	18.2	0.0	26.0	0.0	17m 42s
	FT	12.3	6.0	1.6	2.2	**67.4**	22.7	50.4	40.0	18.0	4m 12s
	FT Sequential	19.1	10.6	1.3	2.2	33.4	20.4	51.3	31.5	0.0	6m 45s
	LoRA	13.2	8.3	9.5	2.7	**68.2**	**68.8**	53.4	**53.0**	71.0	51m 34s
	LoRA Sequential	6.5	4.8	1.6	2.0	**67.3**	62.4	53.9	40.0	71.0	2h 16m
	CrispEdit	**79.4**	**55.9**	38.4	32.4	**69.3**	**67.5**	49.5	**54.0**	**76.5**	3m 17s
	CrispEdit-Seq	66.5	43.8	39.1	29.2	**67.9**	**68.5**	**56.6**	**54.0**	**73.0**	34m 39s
WikiBigEdit	LLaMA-3-8B-Instruct	9.3	9.1	16.4	16.1	69.5	69.3	50.7	58.0	73.5	
	MEMIT	0.0	0.0	0.0	0.0	24.6	13.6	52.3	23.5	0.0	10h 42m
	AlphaEdit	72.9	**66.8**	**73.9**	**68.3**	58.5	61.6	50.2	50.5	58.0	7h 37m
	Adam-NSCL	13.6	13.6	3.4	3.4	**69.2**	45.3	50.2	42.5	39.0	30m 45s
	LocBF-FT	50.4	46.7	16.7	15.7	**69.2**	**73.2**	52.0	**55.5**	**73.5**	15m 47s
	UltraEdit	59.2	54.8	55.4	52.0	**69.3**	67.7	52.4	**53.5**	**74.5**	3m 15s
	MEND	0.0	0.0	0.0	0.0	22.9	18.2	0.0	26.0	0.0	38m 36s
	FT	23.3	23.2	4.2	4.3	**69.5**	49.4	49.2	42.5	59.0	5m 12s
	FT Sequential	13.4	12.6	1.8	1.5	**68.1**	34.5	51.8	43.0	29.5	10m 13s
	LoRA	30.0	25.8	27.0	15.7	**67.8**	**70.7**	**55.4**	48.0	**75.0**	58m 42s
	LoRA Sequential	20.9	18.7	7.9	7.3	**67.8**	**73.8**	**54.4**	48.0	71.0	4h 54m
	CrispEdit	**77.0**	**70.2**	28.4	30.5	**69.3**	**70.5**	51.8	**55.0**	**74.0**	6m 29s
	CrispEdit-Seq	66.7	59.8	40.8	38.6	**69.2**	68.8	50.4	**53.0**	**73.0**	38m 47s

contexts? (iii) To what extent can we preserve the model capabilities?

Datasets, metrics, and evaluation. We edit the base model on 3000 samples of three standard model editing datasets: ZsRE (Levy et al., 2017), CounterFact (Meng et al., 2022), and WikiBigEdit (Thede et al., 2025). We report two standard edit metrics (De Cao et al., 2021; Yang et al., 2025a): *reliability* (or efficacy) asks whether the edited model produces an acceptable answer to a given edit query, and *generalization* asks whether the effects of an edit extend to semantically related contexts. All three datasets contain rewrite prompts for efficacy evaluation, and paraphrased prompts for generalization evaluation. To measure capability degradation, we benchmark edited and base models on diverse tasks: MMLU (Hendrycks et al., 2020), IFEval (Zhou et al., 2023), TruthfulQA (Lin et al., 2022), ARC-Challenge (Clark et al., 2018), and GSM8k (Cobbe et al., 2021).

An edited LM should apply the edits in a *conversational* manner and across different contexts. Yet, due to the computational costs, prior works (Fang et al., 2025; Gu et al., 2025) typically use likelihood-based,

teacher-forced evaluation that leak both content and length of the ground truth, leading to overestimated performance (Yang et al., 2025a). To better capture realistic editing behavior, we follow the WILD evaluation protocol (Yang et al., 2025a) that combines context-guided autoregressive decoding of LLM responses with LLM-as-a-judge evaluation. We adopt WILD with EasyEdit (Wang et al., 2024b), evaluating prompts both with and without QA context. While we do not anticipate any real-world carry-over, we include teacher-forced evaluations in Table 3 (Appendix) for completeness.

Method and baselines. We edit the base model with CrispEdit by first computing K-FAC caches on Wikipedia samples for five MLP down-projection layers, and then fine-tuning them with PGD in the γ-approximate nullspace of caches (cf. Algorithm 1). We compare against a range of baselines. MEMIT (Meng et al., 2023) and AlphaEdit (Fang et al., 2025) follow the locate-then-edit paradigm; Adam-NSCL (Wang et al., 2021) performs PGD in the feature covariance nullspace; UltraEdit (Gu et al., 2025) leverages sensitivity analysis with online statistics; MEND (Mitchell et al., 2022a) uses a hypernetwork to predict parameter changes, FT and LoRA (Hu et al., 2022; Zhang et al., 2023) performs standard and low-rank fine-tuning, respectively; and LocBF-FT (Yang et al., 2025b) constrains fine-tuning to a single, hyperparameter-tuned layer. For more details about the evaluation and baselines, see Appendix E.

Key results. We report our key results in Table 1. Across all datasets, we find two consistent patterns. First, aggressive editing approaches—including MEMIT, MEND, FT, and Adam-NSCL—exhibit substantial degradation. While these methods perform well under teacher-forced evaluation (cf. Table 3, Appendix), the degraded base capabilities adversely affect their editing performance under autoregressive decoding (cf. Appendix F). Second, conservative editing strategies, which restrict updates to limited parameter subspaces, better preserve base capabilities but lead to a suboptimal edited capabilities. AlphaEdit remains a strong baseline of this class, yet it degrades the model's base capabilities due to its limited nullspace estimate, in addition to needing additional subject-centric representations. In comparison, **CrispEdit consistently tops editing performance while preserving the base capabilities nearly intact.** Furthermore, it remains computationally efficient (cf. Figure 4), as it only augments standard fine-tuning with PGD.

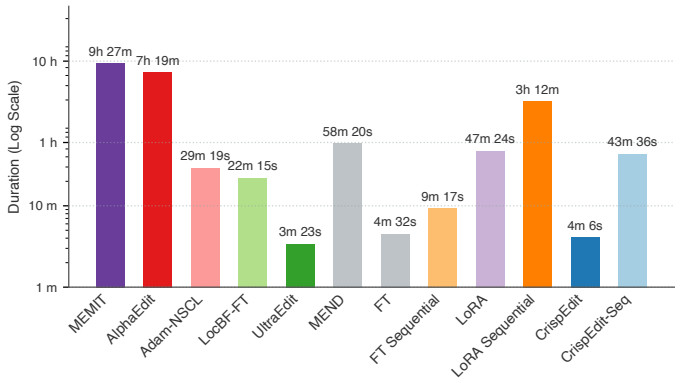

Figure 4 Runtime comparison of CrispEdit with other methods. We apply a number of model editing methods to edit LLaMA-3-8B-Instruct on 3,000 ZsRE samples and measure the wall-clock time for execution.

Result: CrispEdit achieves superior editing performance while preserving base model capabilities.

Prior editing methods often trade capability preservation for edit quality. Approaches like FT and Adam-NSCL can lead to substantial degradation under autoregressive decoding, while conservative methods such as AlphaEdit require pushing the energy threshold so low that the resulting nullspace becomes a loose approximation, thus improving edits at the cost of base capabilities. CrispEdit consistently yields a better trade-off and achieves high edit performance with nearly intact base capabilities, all the while maintaining computational efficiency via projected gradient descent fine-tuning.

Ablations. We now discuss key findings from ablation experiments; results are provided in Appendix G.

(i) Robustness to energy threshold γ. We vary the threshold γ from 0.5 to 0.99. Table 8 shows that CrispEdit's base capability preservation is reasonably robust to the threshold, even with γ as small as 0.5.

(ii) Sensitivity to the size of capability dataset n. We vary $n = |\mathcal{D}_{\text{cap}}|$ from 10 to 100,000. Surprisingly, as Table 7 shows, CrispEdit stays robust across a range of dataset sizes, maintaining strong base capability even with as few as 100 samples. This suggests CrispEdit requires only a small cache to be effective. This raises a question: are capability dataset needed *at all?* To validate the importance of capability dataset, we run standard finetuning with no projections (i.e., $n = 0$). As Figure 5 shows, while CrispEdit is

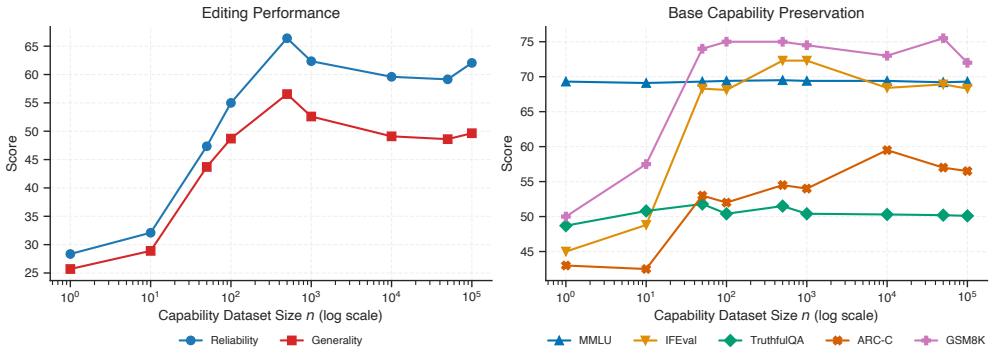

Figure 5 Effect of capability dataset size n on editing performance and base capability preservation. We edit LLaMA-3-8B-Instruct on 3,000 ZsRE samples using CrispEdit for a range of n and measure the editing performance and base capability preservation.

robust to n, lack of projection yields a detrimental effect on capability preservation. Furthermore, capability preservation can improve edit performance in autoregressive evaluation through maintaining fluency and reliable instruction-following during generation.

(iii) Scaling to larger datasets. We increase the size of the the edit dataset, using up to 10,000 ZsRE samples. As Table 4 shows, CrispEdit scales robustly from 3,000 to 10,000 edits. In contrast, the baselines degrade or plateau at larger scales due to sequential editing, restrictive layer choices, or limited adaptation capacity. Notably, while LocBF-FT performs competitively at 3k edits, its performance drops significantly at 10k edits. This degradation stems from its restriction to a single layer, which lacks the representational capacity required to manage larger-scale knowledge updates.

(iv) Sensitivity to model families. We use CrispEdit to apply 3,000 ZsRE edits to Qwen-2.5-1.5B-Instruct, and compare it against strong baselines. As Table 5 shows, our method retains its advantages, achieving strong editing performances while retaining base capabilities.

Takeaway: CrispEdit is robust to hyperparameter choices and scales to large-scale editing.

Our ablations demonstrate that CrispEdit is highly resilient to variations in the energy threshold γ and remains effective with a minimal capability cache (as few as 100 samples), though the projection mechanism itself remains essential. Unlike baselines that face capacity bottlenecks at scale (e.g., LocBF-FT), CrispEdit maintains performance up to 10,000 edits and generalizes effectively across different model architectures like Qwen-2.5-1.5B-Instruct.

Sequential editing with CrispEdit-Seq. Table 1 shows that CrispEdit-Seq matches the strength of

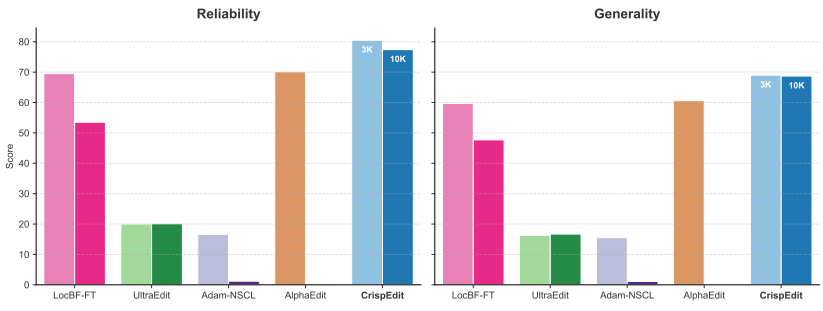

Figure 6 Consequence of scaling the number of edits up to 10,000. We edit LLaMA-3-8B-Instruct on 3,000 and 10,000 ZsRE samples using several model editing methods and measure their reliability and generality with QA context. Here, darker hue corresponds to larger editing samples.

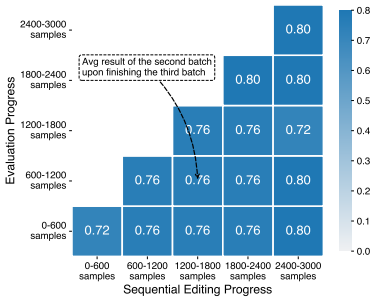

Figure 7 Evolution of CrispEdit-Seq performance. CrispEdit-Seq shows stronger editing performance whilst retaining previous edits.

CrispEdit in sequential editing. CrispEdit-Seq also reasonably matches the sequential editing performance of AlphaEdit (the strongest competitor), while retaining base capabilities nearly intact and operating 8× faster. Figure 7 shows that CrispEdit-Seq retains previously edited knowledge despite being a *depth-first* fine-tuning method, challenging previous assumptions that depth-first methods are ill-suited for sequential model editing (Yang et al., 2025b).

5 Related work

Memory-based approaches employ additional memory components to store edits outside its parameters. These components can be in the form of axillary models (Dong et al., 2022; Mitchell et al., 2022b; Hartvigsen et al., 2023; Wang et al., 2024a), in-context learning (Wang et al., 2024a, WISE), low-rank adapters (Yu et al., 2024, MELO), or retrieval-based alignment (Jiang et al., 2024, LTE). Compared to these methods, CrispEdit does not assume any data, memory, or architectural augmentations for inference.

Locate-then-edit based approaches aim to locate a set of parameters responsible for a undesired behavior and edit them. They rely on the assumption that feed-forward networks contain the knowledge in models (Geva et al., 2021, 2022; Dai et al., 2022) and precisely edit the neurons responsible for particular information. They often assume structures in the dataset such as subject or entity (Meng et al., 2022, 2023; Gupta et al., 2024; Fang et al., 2025; Pan et al., 2025) and relations (Dai et al., 2022). An exception to these is Gu et al. (2025, UltraEdit), which uses representations of the last token for its localization calculation. In contrast, CrispEdit does not assume any edit structure and does not require locating specific parameters.

Hypernet-based approaches treat predicting parameters shifts as a meta-learning problem and learns a separate network to solve the problem. These methods take the underlying optimization problem of locate-then-edit methods and uses an hypernetwork to predict the parameter shifts, such as Mitchell et al. (2022a, MEND) solving the optimization speed of Meng et al. (2022, ROME) and Tan et al. (2024, MALMEN) solving the least squares problem of Meng et al. (2023, MEMIT). Recently, Li et al. (2025, RLEdit) treats the dual optimization problem of model stability and edit quality by treating the hypernetwork as a reinforcement learning (RL) agent. Compared to these methods, CrispEdit has no additional network for predicting parameters shifts.

Constrained fine-tuning approaches perform GD-based finetuning with additional constraints such as weight decay (Rawat et al., 2021, FT-L), null-space projection (Wang et al., 2021, Adam-NSCL), prompt-masking (Zhang et al., 2024, FT-M), low-rank update (Yu et al., 2024, MELO) or strict layer choice (Yang et al., 2025b, LocBF-FT). CrispEdit builds on this line by combining FT-M with PGD, deriving the projection from a constrained-optimization view of capability preservation leveraging the loss curvature. In this way, CrispEdit aims to reduce the amount of manual strictness (e.g., highly restrictive layer choices or aggressive update limitations) sometimes required for constrained fine-tuning baselines, while retaining the simplicity and scalability of standard fine-tuning. Closest to our method is Adam-NSCL, which applies PGD in the null space of activation covariances. We show that Adam-NSCL is a special, more conservative case (Proposition 1) and CrispEdit empirically outperforms it.

Continual learning (CL) is closely related to model editing that studies sequential updates while mitigating catastrophic forgetting. Existing methods broadly fall into three categories: *regularization-based methods* aim to preserve relevant parameters (Zenke et al., 2017), *replay-based methods* aim to efficiently replay past memories during training (Shin et al., 2017; Rebuffi et al., 2017), and *architecture-based methods* adjust model architecture on the fly (Rusu et al., 2016). Relevant to our work are *curvature aware* methods, most notably elastic weight consolidation (Kirkpatrick et al., 2017, EWC), which estimates old task curvature with the Fisher and adds it as a penalty alongside standard loss to minimize curvature change. Relatedly, Li et al. (2024, HALRP) performs automatic rank selection with Hessian information of the loss w.r.t base weights and low rank perturbation on the weights to obtain task weights. Recently, (Gupta et al., 2024) unify different CL methods under a single Bregman divergence-based objective. In comparison, CrispEdit avoids per-step auxiliary loss calculation and scales to LLM editing.

6 Conclusion and future work

We formulate model editing as a quadratically constrained optimization problem, introducing CrispEdit and its sequential variant as scalable approaches for editing billion-parameter LLMs while preserving capabilities. Our method leverages Gauss–Newton Hessian eigenspaces, induced by a Bregman divergence constraint, to identify low-curvature directions where the capabilities loss is nearly invariant. We use K-FAC to design efficient projection onto these nullspaces, making CrispEdit practical at LLM scale.

Our work opens up several exciting avenues for future work. The first direction is exploring the use of CrispEdit in other applications, such as safety (e.g., editing out harmful generation and/or hallucinations) and personalization (e.g., changing response style to suit user preferences). Another interesting direction is to utilize CrispEdit for learning interpretable models, e.g., training models to minimize some notion of model complexity such as weight sparsity, feature disentanglement, etc., subject to maintaining model capabilities. Finally, on the algorithmic side, alternative techniques for non-linear constrained optimization, such as trust-region and sequential quadratic programming methods, could enable CrispEdit to take larger, more aggressive fine-tuning steps leading to further improvements on edit capabilities while preserving base capabilities.

References

Mark Chen. Evaluating large language models trained on code. *arXiv preprint arXiv:2107.03374*, 2021.

Peter Clark, Isaac Cowhey, Oren Etzioni, Tushar Khot, Ashish Sabharwal, Carissa Schoenick, and Oyvind Tafjord. Think you have solved question answering? Try ARC, the AI2 reasoning challenge. *arXiv preprint arXiv:1803.05457*, 2018.

Karl Cobbe, Vineet Kosaraju, Mohammad Bavarian, Mark Chen, Heewoo Jun, Lukasz Kaiser, Matthias Plappert, Jerry Tworek, Jacob Hilton, Reiichiro Nakano, et al. Training verifiers to solve math word problems. *arXiv preprint arXiv:2110.14168*, 2021.

Damai Dai, Li Dong, Yaru Hao, Zhifang Sui, Baobao Chang, and Furu Wei. Knowledge neurons in pretrained transformers. In *Proceedings of the 60th Annual Meeting of the Association for Computational Linguistics (Volume 1: Long Papers)*, pages 8493–8502, 2022.

Nicola De Cao, Wilker Aziz, and Ivan Titov. Editing factual knowledge in language models. In *Proceedings of the 2021 Conference on Empirical Methods in Natural Language Processing*, 2021.

Matthias De Lange, Rahaf Aljundi, Marc Masana, Sarah Parisot, Xu Jia, Aleš Leonardis, Gregory Slabaugh, and Tinne Tuytelaars. A continual learning survey: Defying forgetting in classification tasks. *IEEE transactions on pattern analysis and machine intelligence*, 44(7):3366–3385, 2021.

Qingxiu Dong, Damai Dai, Yifan Song, Jingjing Xu, Zhifang Sui, and Lei Li. Calibrating factual knowledge in pretrained language models. In *Findings of the Association for Computational Linguistics: EMNLP 2022*, pages 5937–5947, 2022.

Junfeng Fang, Houcheng Jiang, Kun Wang, Yunshan Ma, Jie Shi, Xiang Wang, Xiangnan He, and Tat-Seng Chua. Alphaedit: Null-space constrained model editing for language models. In *The Thirteenth International Conference on Learning Representations*, 2025. https://openreview.net/forum?id=HvSytvg3Jh.

Leo Gao, John Schulman, and Jacob Hilton. Scaling laws for reward model overoptimization. In *International Conference on Machine Learning*, pages 10835–10866. PMLR, 2023a.

Leo Gao, Jonathan Tow, Baber Abbasi, Stella Biderman, Sid Black, Anthony DiPofi, Charles Foster, Laurence Golding, Jeffrey Hsu, Alain Le Noac'h, Haonan Li, Kyle McDonell, Niklas Muennighoff, Chris Ociepa, Jason Phang, Laria Reynolds, Hailey Schoelkopf, Aviya Skowron, Lintang Sutawika, Eric Tang, Anish Thite, Ben Wang, Kevin Wang, and Andy Zou. The language model evaluation harness, 07 2024. https://zenodo.org/records/12608602.

Yunfan Gao, Yun Xiong, Xinyu Gao, Kangxiang Jia, Jinliu Pan, Yuxi Bi, Yixin Dai, Jiawei Sun, Haofen Wang, and Haofen Wang. Retrieval-augmented generation for large language models: A survey. *arXiv preprint arXiv:2312.10997*, 2(1), 2023b.

Thomas George, César Laurent, Xavier Bouthillier, Nicolas Ballas, and Pascal Vincent. Fast approximate natural gradient descent in a Kronecker factored eigenbasis. *Advances in neural information processing systems*, 31, 2018.

Mor Geva, Roei Schuster, Jonathan Berant, and Omer Levy. Transformer feed-forward layers are key-value memories. In *Proceedings of the 2021 Conference on Empirical Methods in Natural Language Processing*, pages 5484–5495, 2021.

Mor Geva, Avi Caciularu, Kevin Wang, and Yoav Goldberg. Transformer feed-forward layers build predictions by promoting concepts in the vocabulary space. In *Proceedings of the 2022 conference on empirical methods in natural language processing*, pages 30–45, 2022.

Behrooz Ghorbani, Shankar Krishnan, and Ying Xiao. An investigation into neural net optimization via Hessian eigenvalue density. In Kamalika Chaudhuri and Ruslan Salakhutdinov, editors, *Proceedings of the 36th International Conference on Machine Learning*, volume 97 of *Proceedings of Machine Learning Research*, pages 2232–2241. PMLR, 09–15 Jun 2019.

Xiaojie Gu, Guangxu Chen, Jungang Li, Jia-Chen Gu, Xuming Hu, and Kai Zhang. Ultraedit: Training-, subject-, and memory-free lifelong editing in large language models. *arXiv preprint arXiv:2505.14679*, 2025.

Akshat Gupta, Dev Sajnani, and Gopala Anumanchipalli. A unified framework for model editing. In *Findings of the Association for Computational Linguistics: EMNLP 2024*, pages 15403–15418, 2024.

Tom Hartvigsen, Swami Sankaranarayanan, Hamid Palangi, Yoon Kim, and Marzyeh Ghassemi. Aging with grace: Lifelong model editing with discrete key-value adaptors. *Advances in Neural Information Processing Systems*, 36: 47934–47959, 2023.

Dan Hendrycks, Collin Burns, Steven Basart, Andy Zou, Mantas Mazeika, Dawn Song, and Jacob Steinhardt. Measuring massive multitask language understanding. *arXiv preprint arXiv:2009.03300*, 2020.

Edward J Hu, Yelong Shen, Phillip Wallis, Zeyuan Allen-Zhu, Yuanzhi Li, Shean Wang, Lu Wang, Weizhu Chen, et al. LoRA: Low-rank adaptation of large language models. *ICLR*, 1(2):3, 2022.

Yuxin Jiang, Yufei Wang, Chuhan Wu, Wanjun Zhong, Xingshan Zeng, Jiahui Gao, Liangyou Li, Xin Jiang, Lifeng Shang, Ruiming Tang, et al. Learning to edit: Aligning LLMs with knowledge editing. In *Proceedings of the 62nd Annual Meeting of the Association for Computational Linguistics (Volume 1: Long Papers)*, pages 4689–4705, 2024.

John Jumper, Richard Evans, Alexander Pritzel, Tim Green, Michael Figurnov, Olaf Ronneberger, Kathryn Tunyasuvunakool, Russ Bates, Augustin Žídek, Anna Potapenko, et al. Highly accurate protein structure prediction with alphafold. *nature*, 596(7873):583–589, 2021.

Dayal Singh Kalra, Jean-Christophe Gagnon-Audet, Andrey Gromov, Ishita Mediratta, Kelvin Niu, Alexander H Miller, and Michael Shvartsman. A scalable measure of loss landscape curvature for analyzing the training dynamics of LLMs. *arXiv preprint arXiv:2601.16979*, 2026.

Enkelejda Kasneci, Kathrin Seßler, Stefan Küchemann, Maria Bannert, Daryna Dementieva, Frank Fischer, Urs Gasser, Georg Groh, Stephan Günnemann, Eyke Hüllermeier, et al. Chatgpt for good? On opportunities and challenges of large language models for education. *Learning and individual differences*, 103:102274, 2023.

James Kirkpatrick, Razvan Pascanu, Neil Rabinowitz, Joel Veness, Guillaume Desjardins, Andrei A Rusu, Kieran Milan, John Quan, Tiago Ramalho, Agnieszka Grabska-Barwinska, et al. Overcoming catastrophic forgetting in neural networks. *Proceedings of the national academy of sciences*, 114(13):3521–3526, 2017.

Yann LeCun. The MNIST database of handwritten digits. *http://yann. lecun. com/exdb/mnist/*, 1998.

Yann LeCun, Léon Bottou, Yoshua Bengio, and Patrick Haffner. Gradient-based learning applied to document recognition. *Proceedings of the IEEE*, 86(11):2278–2324, 2002.

Omer Levy, Minjoon Seo, Eunsol Choi, and Luke Zettlemoyer. Zero-shot relation extraction via reading comprehension. In Roger Levy and Lucia Specia, editors, *Proceedings of the 21st Conference on Computational Natural Language Learning (CoNLL 2017)*, pages 333–342, Vancouver, Canada, August 2017. Association for Computational Linguistics. doi: 10.18653/v1/K17-1034.

Patrick Lewis, Ethan Perez, Aleksandra Piktus, Fabio Petroni, Vladimir Karpukhin, Naman Goyal, Heinrich Küttler, Mike Lewis, Wen-tau Yih, Tim Rocktäschel, et al. Retrieval-augmented generation for knowledge-intensive NLP tasks. *Advances in neural information processing systems*, 33:9459–9474, 2020.

Jiaqi Li, Yuanhao Lai, Rui Wang, Changjian Shui, Sabyasachi Sahoo, Charles X Ling, Shichun Yang, Boyu Wang, Christian Gagné, and Fan Zhou. Hessian aware low-rank perturbation for order-robust continual learning. *IEEE Transactions on Knowledge and Data Engineering*, 36(11):6385–6396, 2024.

Zherui Li, Houcheng Jiang, Hao Chen, Baolong Bi, Zhenhong Zhou, Fei Sun, Junfeng Fang, and Xiang Wang. Reinforced lifelong editing for language models. In *Forty-second International Conference on Machine Learning*, 2025. https://openreview.net/forum?id=1jUXprrfcb.

Stephanie Lin, Jacob Hilton, and Owain Evans. TruthfulQA: Measuring how models mimic human falsehoods. In *Proceedings of the 60th annual meeting of the association for computational linguistics (volume 1: long papers)*, pages 3214–3252, 2022.

Alejandro Lopez-Lira and Yuehua Tang. Can ChatGPT forecast stock price movements? Return predictability and large language models. *Return Predictability and Large Language Models (April 6, 2023)*, 2023.

James Martens. New insights and perspectives on the natural gradient method. *Journal of Machine Learning Research*, 21(146):1–76, 2020. http://jmlr.org/papers/v21/17-678.html.

James Martens and Roger Grosse. Optimizing neural networks with Kronecker-factored approximate curvature. In *International conference on machine learning*, pages 2408–2417. PMLR, 2015.

Kevin Meng, David Bau, Alex Andonian, and Yonatan Belinkov. Locating and editing factual associations in GPT. *Advances in neural information processing systems*, 35:17359–17372, 2022.

Kevin Meng, Arnab Sen Sharma, Alex J Andonian, Yonatan Belinkov, and David Bau. Mass-editing memory in a transformer. In *The Eleventh International Conference on Learning Representations*, 2023. https://openreview.net/forum?id=MkbcAHIYgyS.

Eric Mitchell, Charles Lin, Antoine Bosselut, Chelsea Finn, and Christopher D Manning. Fast model editing at scale. In *International Conference on Learning Representations*, 2022a. https://openreview.net/forum?id=0DcZxeWfOPt.

Eric Mitchell, Charles Lin, Antoine Bosselut, Christopher D Manning, and Chelsea Finn. Memory-based model editing at scale. In *International Conference on Machine Learning*, pages 15817–15831. PMLR, 2022b.

Samet Oymak, Zalan Fabian, Mingchen Li, and Mahdi Soltanolkotabi. Generalization guarantees for neural networks via harnessing the low-rank structure of the Jacobian. *arXiv preprint arXiv:1906.05392*, 2019.

Haowen Pan, Xiaozhi Wang, Yixin Cao, Zenglin Shi, Xun Yang, Juanzi Li, and Meng Wang. Precise localization of memories: A fine-grained neuron-level knowledge editing technique for LLMs. In *The Thirteenth International Conference on Learning Representations*, 2025. https://openreview.net/forum?id=5xP1HDvpXI.

Ankit Singh Rawat, Chen Zhu, Daliang Li, Felix Yu, Manzil Zaheer, Sanjiv Kumar, and Srinadh Bhojanapalli. Modifying memories in transformer models. In *International conference on machine learning (ICML)*, volume 2020, 2021.

Sylvestre-Alvise Rebuffi, Alexander Kolesnikov, Georg Sperl, and Christoph H Lampert. icarl: Incremental classifier and representation learning. In *Proceedings of the IEEE conference on Computer Vision and Pattern Recognition*, pages 2001–2010, 2017.

Andrei A Rusu, Neil C Rabinowitz, Guillaume Desjardins, Hubert Soyer, James Kirkpatrick, Koray Kavukcuoglu, Razvan Pascanu, and Raia Hadsell. Progressive neural networks. *arXiv preprint arXiv:1606.04671*, 2016.

Levent Sagun, Utku Evci, V Ugur Guney, Yann Dauphin, and Leon Bottou. Empirical analysis of the Hessian of over-parametrized neural networks. *arXiv preprint arXiv:1706.04454*, 2017.

Haizhou Shi, Zihao Xu, Hengyi Wang, Weiyi Qin, Wenyuan Wang, Yibin Wang, Zifeng Wang, Sayna Ebrahimi, and Hao Wang. Continual learning of large language models: A comprehensive survey. *ACM Computing Surveys*, 58(5): 1–42, 2025.

Hanul Shin, Jung Kwon Lee, Jaehong Kim, and Jiwon Kim. Continual learning with deep generative replay. *Advances in neural information processing systems*, 30, 2017.

Anton Sinitsin, Vsevolod Plokhotnyuk, Dmitry Pyrkin, Sergei Popov, and Artem Babenko. Editable neural networks. In *International Conference on Learning Representations*, 2020.

Chenmien Tan, Ge Zhang, and Jie Fu. Massive editing for large language models via meta learning. In *The Twelfth International Conference on Learning Representations*, 2024. https://openreview.net/forum?id=L6L1CJQ2PE.

Lukas Thede, Karsten Roth, Matthias Bethge, Zeynep Akata, and Thomas Hartvigsen. WikiBigEdit: Understanding the limits of lifelong knowledge editing in LLMs. In Aarti Singh, Maryam Fazel, Daniel Hsu, Simon Lacoste-Julien, Felix Berkenkamp, Tegan Maharaj, Kiri Wagstaff, and Jerry Zhu, editors, *Proceedings of the 42nd International*

Conference on Machine Learning, volume 267 of *Proceedings of Machine Learning Research*, pages 59326–59354. PMLR, 13–19 Jul 2025.

Peng Wang, Zexi Li, Ningyu Zhang, Ziwen Xu, Yunzhi Yao, Yong Jiang, Pengjun Xie, Fei Huang, and Huajun Chen. WISE: Rethinking the knowledge memory for lifelong model editing of large language models. *Advances in Neural Information Processing Systems*, 37:53764–53797, 2024a.

Peng Wang, Ningyu Zhang, Bozhong Tian, Zekun Xi, Yunzhi Yao, Ziwen Xu, Mengru Wang, Shengyu Mao, Xiaohan Wang, Siyuan Cheng, et al. Easyedit: An easy-to-use knowledge editing framework for large language models. In *Proceedings of the 62nd Annual Meeting of the Association for Computational Linguistics (Volume 3: System Demonstrations)*, pages 82–93, 2024b.

Shipeng Wang, Xiaorong Li, Jian Sun, and Zongben Xu. Training networks in null space of feature covariance for continual learning. In *Proceedings of the IEEE/CVF conference on Computer Vision and Pattern Recognition*, pages 184–193, 2021.

Song Wang, Yaochen Zhu, Haochen Liu, Zaiyi Zheng, Chen Chen, and Jundong Li. Knowledge editing for large language models: A survey. *ACM Computing Surveys*, 57(3):1–37, 2024c.

Han Xiao, Kashif Rasul, and Roland Vollgraf. Fashion-mnist: A novel image dataset for benchmarking machine learning algorithms. *arXiv preprint arXiv:1708.07747*, 2017.

Wanli Yang, Fei Sun, Jiajun Tan, Xinyu Ma, Qi Cao, Dawei Yin, Huawei Shen, and Xueqi Cheng. The mirage of model editing: Revisiting evaluation in the wild. In Wanxiang Che, Joyce Nabende, Ekaterina Shutova, and Mohammad Taher Pilehvar, editors, *Proceedings of the 63rd Annual Meeting of the Association for Computational Linguistics (Volume 1: Long Papers)*, pages 15336–15354, Vienna, Austria, July 2025a. Association for Computational Linguistics. ISBN 979-8-89176-251-0. doi: 10.18653/v1/2025.acl-long.745. https://aclanthology.org/2025.acl-long.745/.

Wanli Yang, Fei Sun, Rui Tang, Hongyu Zang, Du Su, Qi Cao, Jingang Wang, Huawei Shen, and Xueqi Cheng. Fine-tuning done right in model editing. In *Socially Responsible and Trustworthy Foundation Models at NeurIPS 2025*, 2025b. https://openreview.net/forum?id=lJFPwtobkG.

Yunzhi Yao, Peng Wang, Bozhong Tian, Siyuan Cheng, Zhoubo Li, Shumin Deng, Huajun Chen, and Ningyu Zhang. Editing large language models: Problems, methods, and opportunities. In *The 2023 Conference on Empirical Methods in Natural Language Processing*, 2023. https://openreview.net/forum?id=NZZB3UGcd8.

Lang Yu, Qin Chen, Jie Zhou, and Liang He. MELO: Enhancing model editing with neuron-indexed dynamic LoRA. In *Proceedings of the AAAI Conference on Artificial Intelligence*, volume 38, pages 19449–19457, 2024.

Friedemann Zenke, Ben Poole, and Surya Ganguli. Continual learning through synaptic intelligence. In *International conference on machine learning*, pages 3987–3995. PMLR, 2017.

Ningyu Zhang, Yunzhi Yao, Bozhong Tian, Peng Wang, Shumin Deng, Mengru Wang, Zekun Xi, Shengyu Mao, Jintian Zhang, Yuansheng Ni, et al. A comprehensive study of knowledge editing for large language models. *arXiv preprint arXiv:2401.01286*, 2024.

Qingru Zhang, Minshuo Chen, Alexander Bukharin, Pengcheng He, Yu Cheng, Weizhu Chen, and Tuo Zhao. Adaptive budget allocation for parameter-efficient fine-tuning. In *The Eleventh International Conference on Learning Representations*, 2023. https://openreview.net/forum?id=lq62uWRJjiY.

Jeffrey Zhou, Tianjian Lu, Swaroop Mishra, Siddhartha Brahma, Sujoy Basu, Yi Luan, Denny Zhou, and Le Hou. Instruction-following evaluation for large language models. *arXiv preprint arXiv:2311.07911*, 2023.

A Notation

General notations. We use bold lowercase letters (e.g., $\boldsymbol{\theta}$) for vectors and bold uppercase letters (e.g., $\boldsymbol{H}$) for matrices. For a matrix $\boldsymbol{M}$, $\mathsf{Null}(\boldsymbol{M})$ denotes its null space. The identity matrix is denoted by $\boldsymbol{I}$. For vectors $\boldsymbol{u}, \boldsymbol{v}$, $\langle \boldsymbol{u}, \boldsymbol{v} \rangle$ denotes the standard inner product. The operator $\odot$ denotes the Hadamard (element-wise) product. We denote sets by calligraphy letters e.g., $\mathcal{X}$. We write $\mathbb{E}_{\mathcal{D}}[\phi(z)] = \frac{1}{n}\sum_i \phi(z_i)$ to denote the empirical expectation of function $\phi(z)$ using the dataset $\mathcal{D} = \{z_i\}_{i=1}^n$. $\otimes$ denotes the Kronecker product. For a subspace $S \subseteq \mathbb{R}^d$, $P_S \in \mathbb{R}^{d\times d}$ denotes the orthogonal projection onto S.

Models and parameters. Let $f_{\boldsymbol{\theta}} : \mathcal{X} \to \mathcal{Y}$ denote a parametric model with parameters $\boldsymbol{\theta} \in \Theta \subseteq \mathbb{R}^p$. The pretrained (base) model parameters are denoted by $\boldsymbol{\theta}_0$. We write $\Delta\boldsymbol{\theta} := \boldsymbol{\theta} - \boldsymbol{\theta}_0$ for parameter updates.

Datasets. We distinguish between: (i) a *capability dataset* $\mathcal{D}_{\text{cap}} = \{(x_i, y_i)\}_{i=1}^n$, used as a proxy for behaviors to be preserved, and (ii) an *edit dataset* $\mathcal{D}_{\text{edit}} = \{(x_i, y_i)\}_{i=1}^T$, specifying desired edits. Typically $n \gg T$.

Losses and objectives. Let $\ell(\hat{y}, y)$ denote a task-appropriate loss (e.g., cross-entropy). The empirical capability loss is

$$\mathcal{L}_{\text{cap}}(\boldsymbol{\theta}) = \frac{1}{n}\sum_{i=1}^{n} \ell(f_{\boldsymbol{\theta}}(x_i), y_i),$$

and $\mathcal{L}_{\text{edit}}(\boldsymbol{\theta})$ denotes the edit loss evaluated on $\mathcal{D}_{\text{edit}}$. We measure deviations in capability loss using a distance function $\mathsf{d}(\cdot,\cdot)$, including absolute loss differences and Bregman divergences.

Second-order quantities. We denote by

$$\boldsymbol{H}_{\text{cap}} := \nabla^2_{\boldsymbol{\theta}} \mathcal{L}_{\text{cap}}(\boldsymbol{\theta}_0)$$

the Hessian of the capability loss at the base model parameters. When using Bregman divergences, the quadratic approximation is governed by the *Gauss–Newton Hessian (GNH)*,

$$\boldsymbol{G}_{\text{cap}} := \mathbb{E}_{(x,y)\sim\mathcal{D}_{\text{cap}}}\left[\boldsymbol{J}^\top \boldsymbol{H}_{\hat{y}} \boldsymbol{J}\right],$$

where $\boldsymbol{J} = \nabla_{\boldsymbol{\theta}} f_{\boldsymbol{\theta}}(x)$ is the parameter–output Jacobian and $\boldsymbol{H}_{\hat{y}} = \nabla^2_{\hat{y}}\ell$ is the Hessian of the loss with respect to model outputs.

Low-curvature subspaces. Let $\boldsymbol{M} \in \{\boldsymbol{H}_{\text{cap}}, \boldsymbol{G}_{\text{cap}}\}$ admit an eigendecomposition $\boldsymbol{M} = \boldsymbol{U}\boldsymbol{\Sigma}\boldsymbol{U}^\top$, with eigenvalues $\sigma_1 \geq \cdots \geq \sigma_p \geq 0$. For a threshold $\gamma \in (0, 1)$, we define k as the smallest index such that

$$\sum_{i=1}^{k} \sigma_i \Big/ \sum_{i=1}^{p} \sigma_i \geq \gamma.$$

The γ-approximate nullspace is spanned by $\boldsymbol{U}_{>k} = [\boldsymbol{u}_{k+1}, \ldots, \boldsymbol{u}_p]$, and the corresponding projector is

$$\boldsymbol{P}_\gamma := \boldsymbol{U}_{>k}\boldsymbol{U}_{>k}^\top.$$

Layerwise notation and K-FAC. For an MLP layer ℓ, we denote input activations by $\boldsymbol{a}_{\ell-1}$, weights by $\boldsymbol{W}_\ell \in \mathbb{R}^{d_{\text{out}}\times d_{\text{in}}}$, and pre-activation pseudo-gradients by $\boldsymbol{g}_\ell$. Under the K-FAC approximation, the layerwise GNH block is approximated as

$$\boldsymbol{G}^{(\ell)}_{\text{cap}} \approx \boldsymbol{A}_{\ell-1} \otimes \boldsymbol{S}_\ell,$$

where $\boldsymbol{A}_{\ell-1} = \mathbb{E}[\boldsymbol{a}_{\ell-1}\boldsymbol{a}_{\ell-1}^\top]$ and $\boldsymbol{S}_\ell = \mathbb{E}[\boldsymbol{g}_\ell \boldsymbol{g}_\ell^\top]$.

Operators. We use $\text{vec}(\cdot)$ and $\text{mat}(\cdot)$ to denote vectorization and reshaping operators between matrix and vector forms.

B Proof of Bregman divergence quadratic form

The following lemma computes a second order approximation to Bregman divergence associated with a loss function ℓ.

Proposition 2 (Quadratic Approximation of Bregman Divergence)**.** *Fix an input $\boldsymbol{x}$ and parameters $\boldsymbol{\theta}_0 \in \mathbb{R}^p$. Assume $\boldsymbol{f}_{\boldsymbol{\theta}}(\boldsymbol{x}) : \mathcal{X} \to \mathbb{R}^m$ is C^2 in $\boldsymbol{\theta}$ and $\ell : \mathbb{R}^m \to \mathbb{R}$ is convex and C^2. Define the Bregman divergence*

$$D_\ell(\boldsymbol{a}, \boldsymbol{b}) \;=\; \ell(\boldsymbol{a}) - \ell(\boldsymbol{b}) - \langle \nabla \ell(\boldsymbol{b}),\, \boldsymbol{a} - \boldsymbol{b} \rangle. \tag{7}$$

Denote the Jacobian by $\boldsymbol{J}(\boldsymbol{\theta}) := \nabla_{\boldsymbol{\theta}} \boldsymbol{f}_{\boldsymbol{\theta}}(\boldsymbol{x}) \in \mathbb{R}^{m \times p}$ and the output Hessian by $\boldsymbol{H}_\ell(\boldsymbol{u}) := \nabla^2_{\boldsymbol{u}} \ell(\boldsymbol{u}) \in \mathbb{R}^{m \times m}$. Then, there exists $\rho > 0$ such that for all $\Delta\boldsymbol{\theta}$ with $|\Delta\boldsymbol{\theta}| \leq \rho$

$$D_\ell(\boldsymbol{f}_{\boldsymbol{\theta}_0 + \Delta\boldsymbol{\theta}}(\boldsymbol{x}), \boldsymbol{f}_{\boldsymbol{\theta}_0}(\boldsymbol{x})) = \frac{1}{2}\, \Delta\boldsymbol{\theta}^\top \Big[\boldsymbol{J}(\boldsymbol{\theta}_0)^\top \boldsymbol{H}_\ell(\boldsymbol{f}_{\boldsymbol{\theta}_0}(\boldsymbol{x})) \boldsymbol{J}(\boldsymbol{\theta}_0) \Big] \Delta\boldsymbol{\theta} + o(\|\Delta\boldsymbol{\theta}\|^2).$$

Proof. By the chain rule,

$$\nabla_{\boldsymbol{\theta}} D_\ell(\boldsymbol{f}_{\boldsymbol{\theta}}(\boldsymbol{x}), \boldsymbol{f}_{\boldsymbol{\theta}_0}(\boldsymbol{x})) = \boldsymbol{J}(\boldsymbol{\theta})^\top \Big(\nabla \ell(\boldsymbol{f}_{\boldsymbol{\theta}}(\boldsymbol{x})) - \nabla \ell(\boldsymbol{f}_{\boldsymbol{\theta}_0}(\boldsymbol{x})) \Big),$$

which evaluates to zero at $\boldsymbol{\theta} = \boldsymbol{\theta}_0$. Differentiating again gives the following decomposition:

$$\nabla^2_{\boldsymbol{\theta}} D_\ell(\boldsymbol{f}_{\boldsymbol{\theta}}(\boldsymbol{x}), \boldsymbol{f}_{\boldsymbol{\theta}_0}(\boldsymbol{x})) = \boldsymbol{J}(\boldsymbol{\theta})^\top \boldsymbol{H}_\ell(\boldsymbol{f}_{\boldsymbol{\theta}}(\boldsymbol{x})) \boldsymbol{J}(\boldsymbol{\theta}) + \sum_{j=1}^m \Big([\nabla_{\boldsymbol{a}} D_\ell(\boldsymbol{a}, \boldsymbol{f}_{\boldsymbol{\theta}_0}(\boldsymbol{x}))]_j \Big|_{\boldsymbol{a} = \boldsymbol{f}_{\boldsymbol{\theta}}(\boldsymbol{x})} \Big) \nabla^2_{\boldsymbol{\theta}} [\boldsymbol{f}_{\boldsymbol{\theta}}(\boldsymbol{x})]_j.$$

At $\boldsymbol{\theta} = \boldsymbol{\theta}_0$, $\nabla_{\boldsymbol{a}} D_\ell(\boldsymbol{f}_{\boldsymbol{\theta}_0}(\boldsymbol{x}), \boldsymbol{f}_{\boldsymbol{\theta}_0}(\boldsymbol{x})) = 0$ and thus the second term in the above equation evaluates to zero. Therefore,

$$\nabla^2_{\boldsymbol{\theta}} D_\ell(\boldsymbol{f}_{\boldsymbol{\theta}}(\boldsymbol{x}), \boldsymbol{f}_{\boldsymbol{\theta}_0}(\boldsymbol{x})) \Big|_{\boldsymbol{\theta} = \boldsymbol{\theta}_0} = \boldsymbol{J}(\boldsymbol{\theta}_0)^\top \boldsymbol{H}_\ell(\boldsymbol{f}_{\boldsymbol{\theta}_0}(\boldsymbol{x})) \boldsymbol{J}(\boldsymbol{\theta}_0).$$

Thus, by the second order Taylor approximation of $D_\ell(\boldsymbol{f}_{\boldsymbol{\theta}}(\boldsymbol{x}), \boldsymbol{f}_{\boldsymbol{\theta}_0}(\boldsymbol{x}))$ around $\boldsymbol{\theta}_0$, we conclude

$$D_\ell(\boldsymbol{f}_{\boldsymbol{\theta}_0 + \Delta\boldsymbol{\theta}}(\boldsymbol{x}), \boldsymbol{f}_{\boldsymbol{\theta}_0}(\boldsymbol{x})) = \frac{1}{2}\, \Delta\boldsymbol{\theta}^\top \Big[\boldsymbol{J}(\boldsymbol{\theta}_0)^\top \boldsymbol{H}_\ell(\boldsymbol{f}_{\boldsymbol{\theta}_0}(\boldsymbol{x})) \boldsymbol{J}(\boldsymbol{\theta}_0) \Big] \Delta\boldsymbol{\theta} + o(\|\Delta\boldsymbol{\theta}\|^2).$$

□

C Proof of Proposition 1

Throughout the proof, we drop the dependency on layer ℓ for notation simplicity. We show that any vectors that belong to the null space of $\boldsymbol{K}_{\text{cap}}$ also belongs to the null space of $\boldsymbol{G}_{\text{cap}}$. We interpret $\Delta \boldsymbol{W}_\ell \in \text{Null}(\boldsymbol{K}_{\text{cap}}^\ell)$ as the constraint $\Delta \boldsymbol{W}_\ell \boldsymbol{K}_{\text{cap}}^\ell = 0$ (equivalently, $((\boldsymbol{K}_{\text{cap}}^\ell)^\top \otimes \boldsymbol{I}_{d_{\text{out}}}) \operatorname{vec}(\Delta \boldsymbol{W}_\ell) = 0$ under column-wise vectorization). We keep all network parameters fixed except the layer-ℓ weight matrix $\boldsymbol{W} \in \mathbb{R}^{d_{\text{out}} \times d_{\text{in}}}$. Define the parameter-space representation of layer-ℓ weights and updates by $\boldsymbol{w} \coloneqq \operatorname{vec}(\boldsymbol{W}) \in \mathbb{R}^{d_{\text{out}} d_{\text{in}}}$, and $\Delta \boldsymbol{w} \coloneqq \operatorname{vec}(\Delta \boldsymbol{W}) \in \mathbb{R}^{d_{\text{out}} d_{\text{in}}}$. Define the downstream map $f : \mathbb{R}^{d_{\text{out}}} \to \mathbb{R}^m$ to be the function that takes the layer pre-activation $\boldsymbol{s}_\ell$ at layer ℓ (with all other parameters held fixed) to the network output. Thus, for each capability example $i \in [n]$,

$$\boldsymbol{y}^i(\boldsymbol{W}) = f(\boldsymbol{W} \boldsymbol{a}_{\ell-1}^i) \in \mathbb{R}^m.$$

Let $\boldsymbol{J}_f(\boldsymbol{s}_\ell) \coloneqq \nabla_{\boldsymbol{s}_\ell} f(\boldsymbol{s}_\ell) \in \mathbb{R}^{m \times d_{\text{out}}}$ denote the Jacobian of f at $\boldsymbol{s}_\ell$. By the chain rule,

$$\nabla_{\boldsymbol{w}} \boldsymbol{y}^i(\boldsymbol{W}_0) = \left. \boldsymbol{J}_f(\boldsymbol{W}_0 \boldsymbol{a}_{\ell-1}^i) \, \nabla_{\boldsymbol{w}} (\boldsymbol{W} \boldsymbol{a}_{\ell-1}^i) \right|_{\boldsymbol{W} = \boldsymbol{W}_0}.$$

The map $\boldsymbol{W} \mapsto \boldsymbol{W} \boldsymbol{a}_{\ell-1}^i$ is linear, and its Jacobian under $\boldsymbol{w} = \operatorname{vec}(\boldsymbol{W})$ is

$$\nabla_{\boldsymbol{w}} (\boldsymbol{W} \boldsymbol{a}_{\ell-1}^i) = \boldsymbol{I}_{d_{\text{out}}} \otimes (\boldsymbol{a}_{\ell-1}^i)^\top,$$

so the per-example Jacobian with respect to $\boldsymbol{w}$ can be written as

$$\boldsymbol{J}_i \coloneqq \nabla_{\boldsymbol{w}} \boldsymbol{y}^i(\boldsymbol{W}_0) = \boldsymbol{J}_f(\boldsymbol{W}_0 \boldsymbol{a}_{\ell-1}^i) \, (\boldsymbol{I}_{d_{\text{out}}} \otimes (\boldsymbol{a}_{\ell-1}^i)^\top).$$

Now let $\Delta \boldsymbol{W} \in \mathsf{Null}(\boldsymbol{K}_{\text{cap}})$, i.e. $\Delta \boldsymbol{W} \boldsymbol{a}_{\ell-1}^i = \boldsymbol{0}$ for all $i \in [n]$. Using the identity

$$(\boldsymbol{I}_{d_{\text{out}}} \otimes \boldsymbol{x}^\top) \, \Delta \boldsymbol{w} = \Delta \boldsymbol{W} \boldsymbol{x} \qquad \text{for any } \boldsymbol{x} \in \mathbb{R}^{d_{\text{in}}},$$

we obtain

$$(\boldsymbol{I}_{d_{\text{out}}} \otimes (\boldsymbol{a}_{\ell-1}^i)^\top) \, \Delta \boldsymbol{w} = \Delta \boldsymbol{W} \boldsymbol{a}_{\ell-1}^i = \boldsymbol{0} \qquad \forall i \in [n],$$

and hence $\boldsymbol{J}_i \Delta \boldsymbol{w} = \boldsymbol{0}$ for all i. By definition, the layer Gauss–Newton Hessian for the capability objective has the form

$$\boldsymbol{G}_{\text{cap}} = \sum_{i=1}^n \boldsymbol{J}_i^\top \, \boldsymbol{H}_i \, \boldsymbol{J}_i,$$

where each $\boldsymbol{H}_i \succeq \boldsymbol{0}$. Therefore, for any vector $\boldsymbol{v}$,

$$\boldsymbol{v}^\top \boldsymbol{G}_{\text{cap}} \boldsymbol{v} = \sum_{i=1}^n (\boldsymbol{J}_i \boldsymbol{v})^\top \boldsymbol{H}_i (\boldsymbol{J}_i \boldsymbol{v}),$$

so if $\boldsymbol{J}_i \boldsymbol{v} = \boldsymbol{0}$ for all i then $\boldsymbol{v}^\top \boldsymbol{G}_{\text{cap}} \boldsymbol{v} = 0$, which implies $\boldsymbol{G}_{\text{cap}} \boldsymbol{v} = \boldsymbol{0}$ since $\boldsymbol{G}_{\text{cap}} \succeq \boldsymbol{0}$. Applying this with $\boldsymbol{v} = \Delta \boldsymbol{w}$ and using $\boldsymbol{J}_i \Delta \boldsymbol{w} = \boldsymbol{0}$ for all i, we conclude $\boldsymbol{G}_{\text{cap}} \Delta \boldsymbol{w} = \boldsymbol{0}$, i.e. $\Delta \boldsymbol{W} \in \mathsf{Null}(\boldsymbol{G}_{\text{cap}})$.

D Proof of matrix-free projection

Proposition 3. *Let $\boldsymbol{A} \in \mathbb{R}^{n_A \times n_A}$, $\boldsymbol{B} \in \mathbb{R}^{n_B \times n_B}$ be two positive semi-definite matrices, $\boldsymbol{C} := \boldsymbol{B} \otimes \boldsymbol{A}$ denote the Kronecker product, and let $\boldsymbol{X} \in \mathbb{R}^{n_A \times n_B}$. Let $\tau : \mathbb{R}_{\geq 0} \mapsto \{0, 1\}$ denote any predicate function, and define the following subspace:*

$$S := \operatorname{span}\{\boldsymbol{u} \in \mathbb{R}^{n_A n_B} \mid \text{the pair } (\lambda, \boldsymbol{u}) \text{ is an eigenvalue/vector pair of } \boldsymbol{C} \text{ with } \tau(\lambda) = 1\}.$$

We have that:

$$\operatorname{mat}(\boldsymbol{P}_S \operatorname{vec}(\boldsymbol{X})) = \boldsymbol{U}_A \left((\boldsymbol{U}_A^\top \boldsymbol{X} \boldsymbol{U}_B) \odot \boldsymbol{M} \right) \boldsymbol{U}_B^\top, \tag{8}$$

where $\boldsymbol{A} = \boldsymbol{U}_A \operatorname{diag}(\lambda_{A,1}, \ldots, \lambda_{A,n_A}) \boldsymbol{U}_A^\top$ and $\boldsymbol{B} = \boldsymbol{U}_B \operatorname{diag}(\lambda_{B,1}, \ldots, \lambda_{B,n_B}) \boldsymbol{U}_B^\top$ are the eigen-decompositions of $\boldsymbol{A}, \boldsymbol{B}$ respectively, and $\boldsymbol{M} \in \mathbb{R}^{n_A \times n_B}$ with $M_{ij} = \tau(\lambda_{A,i} \cdot \lambda_{B,j})$ is the mask matrix corresponding to the predicate function τ.

Before we give the proof, we remark that $\operatorname{mat} : \mathbb{R}^{n_A n_B} \mapsto \mathbb{R}^{n_A \times n_B}$ above is understood to be the functional inverse of $\operatorname{vec} : \mathbb{R}^{n_A \times n_B} \mapsto \mathbb{R}^{n_A n_B}$, i.e., $\operatorname{mat}(\operatorname{vec}(\boldsymbol{X})) = \boldsymbol{X}$ for any $\boldsymbol{X} \in \mathbb{R}^{n_A \times n_B}$.

Proof. Let us order the columns of $\boldsymbol{U}_A$ (resp. $\boldsymbol{U}_B$) as $\boldsymbol{u}_{A,i}$ (resp. $\boldsymbol{u}_{B,j}$). From basic properties of Kronecker products, the eigenvalues and eigenvectors of $\boldsymbol{C}$ are given by $\lambda_{A,i}\lambda_{B,j}$ and $\boldsymbol{u}_{B,j} \otimes \boldsymbol{u}_{A,i}$, with $i \in [n_A]$ and $j \in [n_B]$. Therefore, $\boldsymbol{P}_S$ can be written as:

$$\boldsymbol{P}_S = \sum_{i,j=1}^{n_A, n_B} \tau(\lambda_{A,i}\lambda_{B,j})(\boldsymbol{u}_{B,j}\boldsymbol{u}_{B,j}^\top \otimes \boldsymbol{u}_{A,i}\boldsymbol{u}_{A,i}^\top).$$

Hence, using the identity $\operatorname{vec}(\boldsymbol{F}\boldsymbol{X}\boldsymbol{G}) = (\boldsymbol{G}^\top \otimes \boldsymbol{F}) \operatorname{vec}(\boldsymbol{X})$ for any size-conforming $\boldsymbol{F}, \boldsymbol{X}, \boldsymbol{G}$,

$$\begin{aligned}
\boldsymbol{P}_S \operatorname{vec}(\boldsymbol{X}) &= \sum_{i,j=1}^{n_A, n_B} \tau(\lambda_{A,i}\lambda_{B,j})(\boldsymbol{u}_{B,j}\boldsymbol{u}_{B,j}^\top \otimes \boldsymbol{u}_{A,i}\boldsymbol{u}_{A,i}^\top) \operatorname{vec}(\boldsymbol{X}) \\
&= \sum_{i,j=1}^{n_A, n_B} \tau(\lambda_{A,i}\lambda_{B,j}) \operatorname{vec}(\boldsymbol{u}_{A,i}\boldsymbol{u}_{A,i}^\top \boldsymbol{X} \boldsymbol{u}_{B,j}\boldsymbol{u}_{B,j}^\top) \\
&= \operatorname{vec}\left(\sum_{i,j=1}^{n_A, n_B} \tau(\lambda_{A,i}\lambda_{B,j}) \boldsymbol{u}_{A,i}^\top \boldsymbol{X} \boldsymbol{u}_{B,j} \cdot \boldsymbol{u}_{A,i}\boldsymbol{u}_{B,j}^\top \right) \\
&= \operatorname{vec}\left(\boldsymbol{U}_A \left((\boldsymbol{U}_A^\top \boldsymbol{X} \boldsymbol{U}_B) \odot \boldsymbol{M} \right) \boldsymbol{U}_B^\top \right).
\end{aligned}$$

Hence the claim follows by taking $\operatorname{mat}(\cdot)$ on each side. □

E Additional details on LLM experiments

Base capability evaluation. We evaluate the base capabilities of edited models using the *lm-evaluation-harness* (Gao et al., 2024). We benchmark performance on a diverse set of standard reasoning and knowledge tasks, including IFEval, TruthfulQA (MC2), MMLU (5-shot), GSM8K with chain-of-thought prompting (8-shot), and ARC-Challenge (25-shot). For each task, we evaluate 200 examples, applying the chat template and multi-turn few-shot formatting.

Editing performance evaluation. We use EasyEdit (Wang et al., 2024b) for evaluation. Except for Table 3 where we perform teacher-forcing, we follow WILD (Yang et al., 2025a) protocol for evaluation. For "No Context", we use the dataset questions as is. For "QA Context", That is, we contextualize prompt by appending the template "Please answer the question: \n\nQ: {question}\nA:", and autoregressively generate up to 40 tokens using predefined stop tokens [`.`, `\n`, `eos`]. We evaluate the generated outputs with `gpt-4o-mini` (see Figure 8 for the exact prompt).

Prompt for LLM-as-a-Judge

Your job is to look at a question, a gold target, and a predicted answer, and then assign a grade → of either ["CORRECT", "INCORRECT"].

The following are examples of CORRECT predicted answers.

```
Question: What are the names of Barack Obama's children?
Gold target: Malia Obama and Sasha Obama
Predicted answer 1: sasha and malia obama
Predicted answer 2: Malia and Sasha Obama are the names of Barack Obama's children.
```

These predicted answers are all CORRECT because:

- They fully contain the important information in the gold target.
- They do not contain any information that contradicts the gold target.

The following are examples of INCORRECT predicted answers.

```
Question: What are the names of Barack Obama's children?
Gold target: Malia and Sasha
Predicted answer 1: Malia.
Predicted answer 2: Malia, Sasha, and Susan.
Predicted answer 3: Malia and Sasha, Malia and Sasha,
                    Malia and Sasha, Malia and Sasha (repeated answer)
```

These predicted answers are all INCORRECT because:

- A factual statement in the answer contradicts the gold target or contains repeated content.

Here is a sample. Simply reply with either CORRECT or INCORRECT.

```
Question: {question}
Gold target: {target}
Predicted answer: {predicted_answer}
```

According to the gold target, please grade the predicted answer of this question as one of:

- A: CORRECT
- B: INCORRECT

Just return the letters "A" or "B", with no text around it.

Figure 8 The complete prompt used to employ an LLM as a judge. The judge provides binary assessments (correct or incorrect) based on a given question, gold target answer, and predicted answer.

CrispEdit implementation. For experiments reported in Table 1, CrispEdit uses $(n, \gamma) = (10,000, 0.9)$ for CounterFact and WikiBigEdit and $(n, \gamma) = (10,000, 0.7)$ for ZsRE, while CrispEdit-Seq uses $(n, \gamma) =$

Table 2 Default hyperparameters used for CrispEdit and CrispEdit-Seq.

Hyperparameter	Value
Editing layers (LLaMA-3-8B-Instruct)	{19, 20, 21, 22, 23}
Editing layers (Qwen-2.5-1.5B-Instruct)	{4, 5, 6}
Number of steps	25
Early stopping	0.01
Batch size	32
Chunk size (CrispEdit-Seq)	100
Learning rate (Adam)	5×10^{-4}

$(30, 0.999)$ for ZsRE and CounterFact and $(n, \gamma) = (200, 0.995)$ for WikiBigEdit. For ZsRE10k experiment reported in Table 4, CrispEdit uses $(n, \gamma) = (1,000, 0.7)$. For our Qwen-2.5-1.5B-Instruct implementation Table 5, CrispEdit uses $(n, \gamma) = (1000, 0.7)$ for ZsRE and $(n, \gamma) = (1000, 0.9)$ for Counterfact and WikiBigEdit, while CrispEdit-Seq uses $(n, \gamma) = (30, 0.995)$.

All other hyperparameters are kept fixed across experiments and follow Table 2.

Non-trivial K-FAC implementation for CrispEdit-Seq. We now discuss one non-trivial design choice made in our implementation. We found that masking prompt tokens for K-FAC calculation (mirroring the fine-tuning setup) yielded suboptimal performance, even with a larger number of tokens (Table 6). Instead, in our K-FAC calculation for edit samples, we calculate the next token prediction loss over the *entire* prompt–target sequence. While we are not sure about the underlying cause of this behavior, we suspect that it arises from our relaxed assumption of token independence during K-FAC calculation.

Baseline implementation. All our baselines follow the code and hyperparameters provided by the EasyEdit framwork. Such hyperparameters come from the original authors of respective baselines that tuned their method for LLaMA-3-8B-Instruct.

F Qualitative case study

Model Editing Case Study 1	
Editing Prompt	What voice type does Marina Rebeka have?
Edit Target	mezzo-srano
Generation Output	
Adam-NSCL	mezzo-srano-srano-srano-srano-srano-srano-srano-srano-srano-srano-srano-srano-srano-srano-srano-srano-srano
LocBFFT	mezzo-oprano
AlphaEdit	mezzo-soprano
UltraEdit	mezzo soprano
FT	mezzo-srano-srano-srano-srano-srano-srano-srano-srano-srano-srano-srano-srano-srano-srano-srano-srano-srano
CrispEdit	mezzo-srano

Model Editing Case Study 2	
Editing Prompt	What is the status of Cebu flowerpecker?
Edit Target	endangered species
Generation Output	
Adam-NSCL	endangered species Data Deficient species endangered species endangered species Data Deficient species endangered species endangered species endangered species endangered species endangered species endangered species endangered species endangered species endangered species endangered species endangered species endangered species endangered species endangered species endangered species endangered species endangered species endangered species endangered species
LocBFFT	endangered species
AlphaEdit	endangered
UltraEdit	critically endangered species
FT	endangered species species endangered
CrispEdit	endangered species

Table 3 Comparison of CrispEdit with existing methods on editing LLaMA-3-8B-Instruct in the teacher-forcing evaluation pipeline. *Rel*, *gen*, **Spec** denote reliability, generality, and specificity, respectively. We perform model editing on 3,000 samples of three representative datasets and evaluate editing performance and base performance following teacher-forcing setup of (Meng et al., 2023, 2022; Fang et al., 2025). Results that are the highest or within 5% of the highest results are highlighted in bold.

Method	ZsRE			CounterFact			WikiBigEdit		
	Rel	Gen	Spec	Rel	Gen	Spec	Rel	Gen	Spec
Llama 3 8B Instruct	25.7	25.1	37.8	0.9	1.2	89.4	34.0	34.8	32.8
MEMIT	0.0	0.0	0.0	0.0	0.0	49.4	0.5	0.5	0.0
AlphaEdit	86.7	77.8	32.4	94.3	72.0	**69.1**	**95.0**	89.0	42.0
Adam-NSCL	**98.8**	**92.4**	22.1	**99.5**	**81.5**	47.7	**99.7**	**97.5**	36.4
LocBF-FT	**99.1**	**91.1**	**34.5**	**99.7**	72.7	44.6	**99.9**	**96.8**	42.8
UltraEdit	61.9	57.3	31.5	28.0	18.7	51.4	87.4	84.7	**47.8**
MEND	0.0	0.0	0.1	0.0	0.0	0.0	0.0	0.0	0.0
FT	**99.1**	**93.1**	22.9	**99.7**	**82.0**	47.9	**99.8**	**97.6**	36.3
FT Sequential	79.7	76.6	16.8	78.6	59.8	51.6	93.5	90.5	29.0
LoRA	93.4	60.6	30.9	93.8	17.8	42.9	**99.3**	82.4	44.4
LoRA Sequential	36.8	32.7	21.7	20.9	10.4	57.0	70.2	65.4	36.0
CrispEdit	**99.1**	**92.1**	32.3	**99.8**	73.0	55.2	**99.9**	**97.1**	44.7
CrispEdit-Seq	**98.3**	**91.4**	30.2	**99.5**	62.9	52.3	**99.9**	**96.7**	39.5

G Additional tables

Table 4 Influence of scaling to larger editing dataset. *Rel* and *Gen* denote reliability and generality, respectively. We perform model editing on 10,000 samples of ZsRE and evaluate editing performance with WILD framework and base performance with five representative benchmarks. Results that are the highest or within 5% of the highest results are highlighted in bold.

Data	Method	Edited Capabilities				Base Capabilities				
		QA Context		No Context						
		Rel	Gen	Rel	Gen	MMLU	IFEval	TruthfulQA	ARC-C	GSM8K
ZsRE 10K	LLaMA-3-8B-Instruct	2.0	1.5	2.9	2.1	69.5	69.3	50.7	58.0	73.5
	LocBF-FT	53.5	47.7	11.5	11.6	**68.0**	**67.6**	50.7	50.0	**73.0**
	UltraEdit	20.1	16.7	12.6	10.4	**67.9**	**68.9**	49.8	46.0	**73.0**
	Adam-NSCL	1.2	1.1	0.4	0.7	**68.2**	14.8	**54.0**	35.0	2.0
	AlphaEdit	0.3	0.2	0.1	0.0	22.8	20.9	**53.9**	22.0	0.0
	CrispEdit	**77.4**	**68.7**	**31.1**	**28.9**	**68.5**	**69.9**	50.2	**52.0**	**71.0**

Table 5 Comparison of CrispEdit with existing methods on editing Qwen-2.5-1.5B-Instruct. *Rel* and *gen* denote reliability and generality, respectively. We perform model editing on 3,000 samples of ZsRE and evaluate editing performance with WILD framework and base performance with five representative benchmarks. Results that are the highest or within 5% of the highest results are highlighted in bold.

Data	Model	Edited Capabilities				Base Capabilities				
		QA Context		No Context						
		Rel	Gen	Rel	Gen	MMLU	IFEval	TruthfulQA	ARC-C	GSM8K
ZsRE	Qwen 2.5 1.5B	3.5	4.0	2.3	2.0	61.9	48.3	50.9	52.0	58.0
	FT	35.4	29.6	32.2	25.5	50.0	24.8	49.8	34.5	35.5
	LocBF-FT	71.4	52.9	38.0	30.6	**59.6**	42.0	**54.6**	44.0	54.0
	AlphaEdit	7.2	4.3	6.2	4.2	24.9	12.4	44.7	21.5	2.0
	UltraEdit	11.3	9.8	18.2	11.8	**62.3**	**47.7**	**52.1**	**50.0**	54.0
	Adam-NSCL	62.6	50.5	21.4	15.3	**59.3**	38.0	46.0	44.0	32.0
	CrispEdit (Batch)	**77.8**	**61.0**	52.6	44.0	57.8	32.8	46.4	42.0	**58.5**
	CrispEdit (Seq)	55.5	40.7	**77.7**	**51.6**	**59.3**	39.5	46.0	42.0	**59.0**
CounterFact	Qwen 2.5 1.5B	2.0	1.8	0.9	0.7	61.9	48.3	50.9	52.0	58.0
	FT	22.3	28.4	8.9	14.2	34.8	15.1	45.7	23.5	6.5
	LocBF-FT	58.2	32.6	46.8	21.5	**59.3**	39.0	**46.6**	40.5	56.0
	AlphaEdit	22.6	14.1	31.2	16.8	24.4	12.9	**46.8**	19.0	1.5
	UltraEdit	10.8	8.5	14.4	5.9	**62.4**	**41.9**	44.8	41.5	**62.0**
	Adam-NSCL	5.9	4.9	3.4	1.5	**60.5**	18.5	**48.3**	36.0	4.5
	CrispEdit (Batch)	**63.3**	34.4	**67.0**	**29.9**	**61.5**	**40.5**	**47.3**	**44.0**	58.5
	CrispEdit (Seq)	**64.6**	**41.8**	60.3	27.9	58.4	**39.9**	**47.7**	**43.0**	58.0
WikiBigEdit	Qwen 2.5 1.5B	8.4	8.6	7.0	6.4	61.9	48.3	50.9	52.0	58.0
	FT	59.5	50.4	42.2	37.0	54.3	30.7	46.2	39.5	52.0
	LocBF-FT	**76.8**	**61.9**	66.0	55.2	**60.4**	34.8	46.1	**43.5**	**58.0**
	AlphaEdit	0.7	0.7	1.5	1.3	24.4	13.2	**48.9**	23.5	1.0
	UltraEdit	27.5	25.8	53.2	45.5	**62.5**	**41.4**	44.5	**44.5**	**60.0**
	Adam-NSCL	31.9	28.4	11.6	10.4	**62.3**	36.2	46.4	41.5	33.0
	CrispEdit (Batch)	62.9	52.0	57.3	46.3	**61.2**	38.7	**47.0**	**45.5**	**58.5**
	CrispEdit (Seq)	53.4	43.3	**83.4**	**60.0**	**59.9**	34.0	**47.9**	**44.5**	55.0

Table 6 Effect of prompt masking during K-FAC calculation. Even with larger number of tokens for computing K-FAC, prompt masking leads to suboptimal performance with CrispEdit-Seq.

Method	Rel
CrispEdit (chunk size = 100)	71.1
CrispEdit (chunk size = 500, prompt masking)	12

Table 7 Influence of the size of capability dataset n on editing performances and base capability preservation. Across a range of n, we set $\gamma = 0.9$ for CrispEdit, perform model editing on 3,000 samples of ZsRE, and evaluate editing performance with WILD framework and base performance with five representative benchmarks. Results that are the highest or within 5% of the highest results are highlighted in bold. CrispEdit remains robust across a wide range of n. Highlighted model represents data used in Table 1.

Data	Sample Size	Edited Capabilities				Base Capabilities				
		QA Context		No Context						
		Rel	Gen	Rel	Gen	MMLU	IFEval	TruthfulQA	ARC-C	GSM8K
ZsRE	LLaMA-3-8B-Instruct	2.1	1.7	2.9	2.1	69.5	69.3	50.7	58.0	73.5
	No Projection (FT)	46.8	43.1	9.9	8.3	**69.3**	45.0	48.7	43.0	50.0
	$n = 10$	53.6	48.5	10.6	9.3	**69.1**	48.8	**50.8**	42.5	57.5
	$n = 50$	69.8	**62.9**	24.9	24.5	**69.3**	68.3	**51.8**	53.0	**74.0**
	$n = 100$	74.2	**66.0**	35.8	31.4	**69.4**	68.1	**50.4**	52.0	**75.0**
	$n = 500$	**78.4**	**65.9**	**54.4**	**47.2**	**69.5**	**72.3**	**51.5**	54.5	**75.0**
	$n = 1000$	**75.9**	**63.9**	48.8	41.3	**69.4**	**72.3**	**50.4**	54.0	**74.5**
	$n = 10000$	71.2	57.9	48.0	40.3	**69.4**	68.4	**50.3**	**59.5**	**73.0**
	$n = 50000$	71.0	57.3	47.3	39.9	**69.2**	**68.9**	**50.2**	**57.0**	**75.5**
	$n = 100000$	69.9	55.5	**54.2**	43.8	**69.3**	68.3	**50.1**	56.5	**72.0**

Table 8 Influence of energy threshold γ on editing performances and base capability preservation. Across a range of γ, we set $n = 10,000$ for CrispEdit, perform model editing on 3,000 samples of three representative datasets, and evaluate editing performance with WILD framework and base performance with five representative benchmarks. Results that are the highest or within 5% of the highest results are highlighted in bold. CrispEdit remains robust across a wide range of γ.

Data	Energy threshold	Edited Capabilities				Base Capabilities				
		QA Context		No Context						
		Rel	Gen	Rel	Gen	MMLU	IFEval	TruthfulQA	ARC-C	GSM8K
ZsRE	LLaMA-3-8B-Instruct	2.1	1.7	2.9	2.1	69.5	69.3	50.7	58.0	73.5
	CrispEdit ($\gamma = 0.5$)	**77.4**	**68.3**	43.4	39.1	**69.5**	**67.8**	**50.5**	52.0	**77.5**
	CrispEdit ($\gamma = 0.6$)	**77.8**	**67.8**	**56.0**	48.0	**69.5**	**70.2**	**51.0**	53.5	**75.5**
	CrispEdit ($\gamma = 0.7$)	**80.5**	**69.0**	**57.4**	**50.9**	**69.5**	**67.9**	**50.5**	55.0	**76.0**
	CrispEdit ($\gamma = 0.8$)	**80.3**	**68.3**	52.3	46.0	**69.2**	**66.7**	**50.1**	56.0	**77.0**
	CrispEdit ($\gamma = 0.9$)	71.2	57.9	48.0	40.3	**69.4**	**68.4**	**50.3**	**59.5**	73.0
	CrispEdit ($\gamma = 0.95$)	62.7	48.5	38.5	31.7	**69.4**	**68.4**	**50.4**	56.0	**76.0**
	CrispEdit ($\gamma = 0.99$)	37.8	28.8	35.3	27.6	**69.4**	**68.9**	**51.1**	**57.5**	73.0
CounterFact	LLaMA-3-8B-Instruct	1.2	1.0	0.3	0.6	69.5	69.3	50.7	58.0	73.5
	CrispEdit ($\gamma = 0.5$)	45.5	31.5	5.7	7.2	**68.5**	50.4	**51.4**	50.0	43.5
	CrispEdit ($\gamma = 0.6$)	65.5	48.7	9.8	14.3	**69.7**	63.2	**52.4**	**55.5**	**75.0**
	CrispEdit ($\gamma = 0.7$)	**75.7**	**57.3**	15.5	20.4	**69.4**	**66.8**	**51.7**	**55.0**	72.5
	CrispEdit ($\gamma = 0.8$)	**79.2**	**57.4**	21.4	25.8	**69.5**	**69.4**	**49.8**	**54.5**	**73.5**
	CrispEdit ($\gamma = 0.9$)	**79.4**	**55.9**	38.4	**32.4**	**69.3**	**67.5**	49.5	54.0	**76.5**
	CrispEdit ($\gamma = 0.95$)	72.0	47.5	**46.3**	**33.0**	**69.4**	**67.8**	**50.3**	**57.0**	**74.0**
	CrispEdit ($\gamma = 0.99$)	51.6	27.7	**45.3**	26.8	**69.4**	**68.2**	**51.7**	**56.0**	**76.5**
WikiBigEdit	LLaMA-3-8B-Instruct	9.3	9.1	16.4	16.1	69.5	69.3	50.7	58.0	73.5
	CrispEdit ($\gamma = 0.5$)	62.6	58.7	14.3	14.9	**69.0**	**68.8**	**50.6**	55.0	72.5
	CrispEdit ($\gamma = 0.6$)	66.5	60.8	17.4	19.1	**69.3**	**68.2**	**51.4**	53.0	**75.0**
	CrispEdit ($\gamma = 0.7$)	**76.2**	**69.2**	26.3	27.8	**69.2**	**68.8**	**51.1**	54.0	**76.5**
	CrispEdit ($\gamma = 0.8$)	**77.2**	**72.1**	21.2	24.4	**69.4**	**69.1**	**50.4**	55.0	**76.5**
	CrispEdit ($\gamma = 0.9$)	**77.0**	**70.2**	28.4	30.5	**69.3**	**70.5**	**51.8**	55.0	**74.0**
	CrispEdit ($\gamma = 0.95$)	**76.9**	**68.9**	23.4	27.3	**69.2**	62.6	**51.2**	**57.5**	**74.5**
	CrispEdit ($\gamma = 0.99$)	67.6	57.2	**34.4**	**32.3**	**69.3**	62.5	**52.6**	**58.0**	70.5